Projected near-term changes in monsoon precipitation over Peninsular Malaysia in the HighResMIP multi-model ensembles

Climate Dynamics (2023) 60:1151–1171
https://doi.org/10.1007/s00382-022-06363-5

Projected near-term changes in monsoon precipitation over Peninsular Malaysia in the HighResMIP multi-model ensembles

Ju Liang[1] · Mou Leong Tan[2] · Jennifer L. Catto[1] · Matthew K. Hawcroft[3,4] · Kevin I. Hodges[5] · James M. Haywood[1,3]

Received: 7 February 2022 / Accepted: 21 May 2022 / Published online: 25 June 2022

Abstract

Changes in the monsoon season rainfall over Peninsular Malaysia by the mid-21st century are examined using multi-model ensemble data from the CMIP6 HighResMIP experiments. We examine simulations of the present and future climate simulations run under a high emission scenario of greenhouse gases from the Shared Socioeconomic Pathways (SSP5-8.5). The combined effects of horizontal and vertical resolutions on the projected changes in monsoon rainfall and associated environmental fields are investigated by comparing the ensemble mean of the projected changes utilizing appropriate multi-model groupings. The results indicate a projected decrease (by up to 11% near Mersing of eastern Johor, for the period 2031–2050 relative to 1981–2000) in monsoon precipitation along the southeastern coast of Peninsular Malaysia during the northeast monsoon season associated with the projected weakening of the monsoon flow during boreal winter. For the northwestern regions (e.g. Perak) often affected by severe floods, a significant increase in precipitation (by up to 33%) is projected during the southwest monsoon season, partly driven by the projected strengthening of the cross-equatorial flow and the weakened low-level anti-cyclonic shear of winds in boreal summer. However, the magnitudes and signal-to-noise ratios of the projected changes vary considerably with respect to different horizontal and vertical resolutions. Firstly, models with relatively high horizontal and vertical resolutions project a more significant decrease in precipitation during the northeast monsoon season. Secondly, for the southwest monsoon season, models with relatively high horizontal resolutions project larger magnitudes of increases in precipitation over the northern region, while smaller increases are found in simulations with relatively high vertical resolutions. Generally, reduced ensemble spread and increased signal-to-noise ratios are found in simulations at higher horizontal and vertical resolutions, suggesting increased confidence in model projections with increased model resolution.

Keywords Precipitation · Peninsular Malaysia · Model resolution · HighResMIP

1 Introduction

Peninsular Malaysia is located in the north of the western Maritime Continent. The climate of this region features a relatively wet season during boreal winter (from November to February, NDJF) and a dry season in summer (May to August, MJJA). The wet season, usually referred to as the northeast monsoon season, features long-lasting and intense precipitation due to the domination of the transport of warm-moist air by the northeasterly winter monsoon flow from the South China Sea (Johnson and Houze 1987; Chang et al. 2005; Tangang et al. 2008), especially along the east coast with rainfall controlled by the orographic precipitation effect (Juneng et al. 2007). In this season, weather systems such as the northeasterly cold surges (Tangang et al. 2008; Samah et al. 2016) and their interactions with Borneo Vortices (Ooi et al. 2011; Koseki et al. 2014; Paulus and

✉ Ju Liang
J.Liang@exeter.ac.uk

1 College of Engineering, Mathematics and Physical Sciences, University of Exeter, Exeter EX4 4QE, UK

2 GeoInformatic Unit, Geography Section, School of Humanities, Universiti Sains Malaysia, 11800 USM Pulau Pinang, Malaysia

3 Met Office, Exeter EX1 3PB, UK

4 University of Southern Queensland, Toowoomba, QLD 4300, Australia

5 Department of Meteorology, University of Reading, Reading RG6 6ET, UK

Shanas 2017; Liang et al. 2021a) are frequently observed, leading to extreme precipitation in Peninsular Malaysia. Conversely, the dry summer season, usually referred to as the southwest monsoon season, features decreased convective activity of the atmosphere (Chenoli et al. 2018) dominated by the southwesterly monsoon flow. This is associated with the stable anti-cyclonic horizontal winds with relatively strong southwesterly winds to the north of the peninsula (Liang et al. 2021a). In this relatively dry season, however, extreme precipitation events are observed over the northwest and along the southern coast of the peninsula (Suhaila et al. 2010). These are associated with the presence of the southwesterly monsoon flow to the northwest as well as the cross-equatorial southerly flow to the south (Chenoli et al. 2018; Liang et al. 2021a).

In Peninsular Malaysia, damage and fatalities caused by the observed spectrum of hydrological extremes in the main monsoon seasons pose great challenges to local sustainable development (e.g. Chan and Parker 1996; Mohd et al. 2006; Lee and Mohamad 2014; Muqtada et al. 2014). These challenges have become more aggravated and complex in the past four decades as local rain gauge records suggest increasing trends in the occurrence of precipitation extremes across Peninsular Malaysia (Syafrina et al. 2015; Mayowa et al. 2015), which is set in the context of the general increase in the annual total precipitation (Mayowa et al. 2015). This has been highlighted by the recent event of wide-spread flash-floods triggered by an extreme storm in the 2021/22 winter, which affected various densely populated regions of the peninsula including Kelantan, Terengganu, Selangor, Pahang, Perak and Malacca (IFRC 2021).

To address the above-mentioned challenges, the application of climate models plays an important role as they are capable of projecting the possible future changes in precipitation and associated climate extremes in a warmer climate, thereby helping to develop coping strategies associated with future hydrological changes. Studies based on global climate models (GCMs) have suggested significant future changes in annual total precipitation over Peninsular Malaysia. For instance, Tan et al. (2014) used an ensemble of six GCMs to project the changes in precipitation over the Johor River Basin. The study projected a precipitation increase of up to 9% at the Kluang station of the peninsula by the end of the 21st century under the RCP (Representative Concentration Pathway) 4.5 scenario. However, the GCMs used in Tan et al. (2014) demonstrated considerable uncertainties in the magnitudes of such an increase. The study of Endo et al. (2012) has suggested that the uncertainties in the future projection of precipitation over Southeast Asia are possibly linked to the choice of physical parameterization schemes. On the other hand, although there is insufficient evidence to link these uncertainties to the diversity of spatial resolutions in the current CMIP GCMs, the dependence of the GCMs' performance on the model resolutions has been extensively discussed. For example, it is evident that coarse GCM horizontal model resolutions can lead to poorly simulated synoptic scale processes related to precipitation in the tropics (e.g. Yang et al. 2009; McCrary et al. 2014; Roberts et al. 2020; Vannière et al. 2020; Liang et al. 2021a) and consequently limit the model performance in simulating precipitation. Also, climate models with grid spacing greater than 100 km have difficulty in resolving fine-scale atmosphere-orographic interactions (e.g. Smith et al. 2015; Güttler et al. 2015), especially for interactions between the monsoon circulation and the complex land-sea distribution and topography across the western Maritime Continent (Chang et al. 2005). Many studies focusing on Peninsular Malaysia have attempted to address these issues by applying statistical downscaling (Juneng et al. 2010; Nadrah et al. 2011; Amin et al. 2014; Amirabadizadeh et al. 2016; Hassan et al. 2015; Noor et al. 2020) and dynamical downscaling (e.g. Kwan et al. 2014; Shaaban et al. 2011; Chin and Tan 2018; Tan et al. 2019, 2020; Ngai et al. 2020; Tangang et al. 2020). However, downscaling methods have demonstrated considerable uncertainties in the representation of precipitation as their performances are sensitive to both the choice of driving data from the GCMs as well as the internal configurations of the downscaling methods (e.g. Noor et al. 2020; Nguyen-Thuy et al. 2021; Tangang et al. 2020). In addition, there are two main limitations in studies modeling precipitation over Southeast Asia using GCMs. First, the role of model resolution in the projected changes in precipitation has not been sufficiently investigated in this region. Second, the vertical resolution of GCMs have been found to play an important role in the simulation of convective precipitation and its sub-seasonal variability in the tropics (Inness et al. 2001), but this role is frequently ignored.

Based on the High Resolution Model Intercomparison Project (HighResMIP, Haarsma et al. 2016) of CMIP6, our previous evaluation work (Liang et al. 2021b, hereafter L2021) emphasized the important role of increasing horizontal and vertical model resolutions in improving the representation of the historical precipitation climatology over Peninsular Malaysia. This work performed a classification of twenty GCM simulations into different ensemble groups, i.e., low horizontal resolution (Lh), high horizontal resolution (Hh), low vertical resolution (Lv) and high vertical resolution (Hv), which helped to demonstrate the combined effects of horizontal and vertical resolutions on the simulation of precipitation by the GCMs. This work demonstrated improved performance in simulating historical monsoon precipitation over Peninsular Malaysia in the model simulations with higher horizontal and vertical resolutions. However, as most of the current CMIP6 GCMs used for the future climate projections are still at a resolution of the Lh (i.e. grid spacing > 60-km) and Lv (fewer than 80 atmospheric

vertical levels) classes, further investigations are required to understand the uncertainties of these GCMs in simulating the future precipitation changes and how such uncertainties can be reduced by increasing the model resolutions. It is noted that in grouping the GCM simulations by their resolution it is difficult to eliminate the influence of other model configurations (e.g., different dynamical cores and physical parameterizations). However, similar groupings have been used in previous research using CMIP experiments (e.g., Anstey et al. 2013; Gu et al. 2015; Huang et al. 2018; He et al. 2019; Tao et al. 2020) and such groupings are thus considered to be a useful, if imperfect, method for examining the role of model spatial resolution.

Here, the primary motivation of this study is to document the projected near-term changes in precipitation in GCM experiments under a high-level GHG emission scenario and investigate their sensitivities to the changes in both horizontal and vertical GCM resolutions. A brief evaluation of the model performance in simulating precipitation during a 20-year historical period by comparing with multiple precipitation observations and climate reanalysis datasets will be performed to provide an overview of the confidence in the projected changes in precipitation. This study will help understand how state-of-the-art GCM simulations can be used to deliver a more confident projection of the possible future changes in precipitation in this region. The specific aims of the study include:

(a) To assess the sensitivity of the near-term projection of monsoon precipitation by the mid-21st century to changes in model spatial resolution as simulated by the HighResMIP experiments over the domain of Peninsular Malaysia.
(b) To examine how the model uncertainties, quantified by the ensemble spreads and the signal-to-noise ratios (SNR) in different ensemble groups, in the projected precipitation changes vary with the changes in GCM horizontal and vertical resolutions.

The paper continues in Sect. 2 briefly introducing the HighResMIP experiments and the external forcing used for the present and future climate simulations. The data used for model validation and the methodology used for analyses are also described. Section 3 reports the results of the analyses on the resolution dependence of projected near-term precipitation changes by the mid-21st century based on multiple ensembles of HighResMIP GCMs at different model resolutions. Finally, Sect. 4 summarizes the findings and discusses the implications of the study.

2 Data and methods

2.1 The HighResMIP experiments

As an integral protocol of CMIP6 (Eyring et al. 2016), HighResMIP coordinates the use of high-resolution GCM ensembles to promote the understanding of the role played by model resolution in "the simulated mean climate and its variability" as well as the "origins and consequences of systematic model biases" (Haarsma et al. 2016). The GCMs in this protocol provide outputs for both atmosphere-only (i.e. AMIP-style experiments of Tiers 1 and 3) and coupled atmosphere-ocean (Tier 2, named hist-1950 and highres-future) experiments, which help to investigate the role of the atmosphere-ocean coupling processes in climate simulations. This study focuses on the atmosphere-only experiments due to the currently limited data availability of the coupled simulations. The model simulations cover historical (1981–2014) and future (2015–2050) periods. For the sea surface temperature (SST) and sea-ice forcing, the historical simulations (named highresSST-present) are forced by the HadISST2.2.0.0 SST and sea-ice forcing dataset at a resolution of 0.25° (Titchner and Rayner 2014). The future climate simulations (highresSST-future) are forced by a blend of the observed interannual variability derived from the HadISST2.2.0.0 dataset for the period 1960–2014 and the projected SST warming derived from the ensemble mean of the CMIP5 future climate simulations under the RCP8.5 scenario. The future climate simulations are run from 2015 for 36 years forced by a high emission scenario of greenhouse gases from the Shared Socioeconomic Pathways (SSP5-8.5, O'Neill et al. 2014). In this study, the projected near-future changes in precipitation are derived over the future period of 2031–2050 relative to the historical period of 1981–2000, i.e. the earliest and the last 20 years of the data period are compared to demonstrate the precipitation sensitivity to the warming under the high emission scenario.

Eighteen simulations of HighResMIP are used and classified into eight different groups for inter-comparison, i.e. Lh, Hh, Lv, Hv, Lh-Lv, Hh-Lv, Lh-Hv and Hh-Hv. The simulations at grid spacings of greater than 0.6° (~70-km) are classified as the Lh group; and, conversely, those finer than 0.6° are categorized as Hh. As an exception, the low-resolution version of the HiRAM-SIT simulations is classified as Lh, though its grid spacing is finer than 0.5°. This helps to compare the high-resolution simulations with their low-resolution counterparts with the same model configuration so that the effect of horizontal resolution on simulations can be better generalized. The simulations at a vertical resolution (number of atmospheric layers) of fewer (more) than 60 levels are classified as the Lv (Hv) group. About half of the simulations fall into each of the four groups (Lh, Hh, Lv

and Hv). Information on the GCM experiments and their corresponding developers and the classification of resolution groups is summarized in Table 1. Differences from L2021 include the use of the recently released HiRAM-SIT and CMCC-CM2 simulations, while simulations from ECMWF-IFS, IPSL-CM6A, INM-CM5-H and CAMS-CSM1 are not included in this study due to the limited data availability for their future climate simulations.

2.2 Methods for model validation

The ability of the HighResMIP experiments to simulate the monsoon precipitation over Peninsular Malaysia has been reported in detail by L2021. As the multi-model GCM ensembles used here are slightly different, a brief discussion on the performance of the experiments that simulate monsoon precipitation in Peninsular Malaysia is reported prior to the future projection analyses.

Three different historical precipitation datasets and four different reanalysis datasets are used as validation data to verify the ability of the HighResMIP GCMs to simulate precipitation and associated large-scale environments in Peninsular Malaysia for the historical baseline period (1981–2000). Due to the limited temporal length of data, the Integrated Multi-satellitE Retrievals for Global Precipitation Measurement (Huffman et al. 2015) used by L2021 is replaced by the satellite observed precipitation data from the Climate Hazards Group InfraRed Precipitation with Station (CHIRPS, Peterson et al. 2015) at 0.05° × 0.05° spatial resolution. Information on all the model validation data is summarized in Table 2. All the precipitation data from the different observation datasets and GCMs are linearly interpolated to the 0.1° × 0.1° standard grids over Peninsular Malaysia, where the inter-comparison of precipitation among the different models and observational data is made. An inter-comparison of the monsoon precipitation amount during the northeast (NDJF) and southwest monsoon (MJJA) seasons is made for the observed precipitation data and the GCM simulations. Other methods, such as the calculation of extreme precipitation rate and the statistical metrics to evaluate the performance of each model group with respect to the observed precipitation datasets are described in L2021.

2.3 Analysis of the projected future changes

The near-term projected changes in precipitation and extreme precipitation rate (i.e. the 95th percentile of daily precipitation on wet days with precipitation > 0.1 mm/day) in terms of multi-model ensemble mean (MME) for each resolution group are derived over the future period of 2031–2050 relative to the historical baseline period of 1981–2000. For different model groups, projected changes in precipitation and extreme precipitation rate are quantified by the relative change (unit: %) between the projection period and baseline period. In addition, box-and-whisker plots are used to show the projected changes in the annual cycle of precipitation

Table 1 Summary of the used CMIP6 HighResMIP experiments in this study

Label no.	Modeling organizations	Model Name	Horizontal resolution (Longitude×Latitude)	Atmospheric vertical levels	Hori. res. categ.	Vert. res. categ.
1	The UK Met Office Hadley Centre for Climate Change	HadGEM3-GC31	1.875° × 1.25°	85	Lh	Hv
2			0.83° × 0.56°		Lh	Hv
3			0.35° × 0.23°		Hh	Hv
4	French National Centre for Meteorological Research	CNRM-CM6-1	1.406° × 1.406°	91	Lh	Hv
5			0.5° × 0.5°		Hh	Hv
6	27 institutes in Europe (Haarsma et al. 2020)	EC-Earth3P	0.703° × 0.703°	91	Lh	Hv
7			0.352° × 0.352°		Hh	Hv
8	Meteorological Research Institute (Japan)	MRI-AGCM3-2	0.563° × 0.563°	60	Lh	Hv
9			0.188° × 0.188°		Hh	Hv
10	Japan Agency for Marine-Earth Science and Technology	NICAM16	0.563° × 0.563°	38	Lh	Lv
11			0.281° × 0.281°		Hh	Lv
12	Institute of Atmospheric Physics/ Chinese Academy of Sciences	FGOALS-f3	1.25° × 1°	32	Lh	Lv
13			0.25° × 0.25°		Hh	Lv
14	Geophysical Fluid Dynamics Laboratory/ NOAA (U.S.)	GFDL-CM4C192	0.625° × 0.5°	33	Lh	Lv
15		HiRAM-SIT	0.5° × 0.5°	32	Lh	Lv
16			0.234° × 0.234°		Hh	Lv
17	Euro-Mediterranean Center on Climate Change (Italy)	CMCC-CM2	1.25° × 0.938°	26	Lh	Lv
18			0.313° × 0.234°		Hh	Lv

Table 2 Summary of the used model validation data

Organizations	Dataset name	Horizontal resolution (Longitude × Latitude)	References
Observed daily precipitation datasets			
Malaysian Meteorological Department (MMD)	Observed daily precipitation from 53 rain gauge stations over Peninsular Malaysia	N/A	Daud (2010)
Research Institute for Humanity and Nature	Asian Precipitation- Highly-Resolved Observational Data Integration Towards Evaluation (APHRODITE)	0.25° × 0.25°	Yatagai et al. (2014)
Climate Hazards Center and United States Geological Survey	Climate Hazards Group InfraRed Precipitation with Station (CHIRPS)	0.05° × 0.05°	Peterson et al. (2015)

Organizations	Dataset name	Horizontal resolution (Longitude × Latitude)	Atmospheric vertical levels	References
Climate reanalysis datasets				
European Centre for Medium-Range Weather Forecasts	ERA5	0.25° × 0.25°	137	Hersbach et al. (2020)
The Japan Meteorological Agency	JRA-55	0.5° × 0.5°	60	Kobayashi et al. (2015)
The National Aeronautics and Space Administration, U.S.	MERRA-2	0.5° × 0.625°	72	Gelaro et al. (2017)
National Centers for Environmental Prediction, U.S.	NCEP-CFSR	0.312° × 0.312°	91	Saha et al. (2010)

over the west and east coast stations (Fig. 1) of Peninsular Malaysia and their uncertainties.

The SNR of the projected changes is calculated for each ensemble group to quantify the uncertainties of the multi-model GCM ensembles. Following the method of Kim et al. (2019), Ge et al. (2021) and Nath and Luo (2021), SNR (unit: %) is calculated as:

$$SNR = \frac{X}{\sigma} \times 100, \quad (1)$$

where X is the MME mean of the projected relative changes and σ is the ensemble spread, i.e. one standard deviation of the projected relative changes from each ensemble member.

3 Results

3.1 Simulations for the baseline period

In this section we briefly discuss the performance of the selected ensemble members in simulating monsoon precipitation for the period 1981–2000 based on their comparison with those from the observations, i.e. the daily observations at rain gauge stations from the Malaysian Meteorological Department (MMD), Asian Precipitation-Highly-Resolved Observational Data Integration Towards Evaluation (APHRODITE) and CHIRPS.

Due to the differing annual precipitation cycles between the east coast and west coast of Peninsular Malaysia (Wong et al. 2009), we first evaluate if the ensembles of different resolution groups can capture such distinct and differentiated precipitation regimes in this region. For selected stations along the east coast (Fig. 2a), the observed precipitation datasets indicate a distinct peak of precipitation from November to December. All model groupings reasonably capture a precipitation peak in boreal winter; however, all the ensembles except Hh-Hv simulate an earlier precipitation peak (by about a month). All the simulations underestimate the precipitation along the east coast for the NDJF northeast monsoon season, particularly for December. On the other hand, along the west coast, there are two precipitation peaks in April and October according to the observed precipitation (Fig. 2b). Such a double-peak in the monthly distribution is simulated reasonably well by all the model groups; however, Lv and Hh-Lv simulate a peak in November that is one month later than the observation and they exhibit pronounced overestimation of precipitation for both the peaks, though these biases are apparently improved by increases in vertical resolution. No apparent improvement is found in Hh when compared with Lh. These results are generally consistent with L2021 though the selected ensemble members differ. For instance, the underestimated peak precipitation along the east coast is consistent with the overly weak northeasterly monsoon flow during winter for most of the resolution groups as presented by L2021. In addition, the overestimated precipitation in simulations at relatively low vertical resolution can be partly attributed to the overly strong vertical ascent at 850 hPa in different monsoon seasons.

Figure 2c–f shows the Taylor diagrams for a statistical evaluation of the simulated distributions of accumulation and extreme precipitation rate (in terms of the 95th percentile of daily precipitation) compared with the mean observed patterns from MMD, APHRODITE and

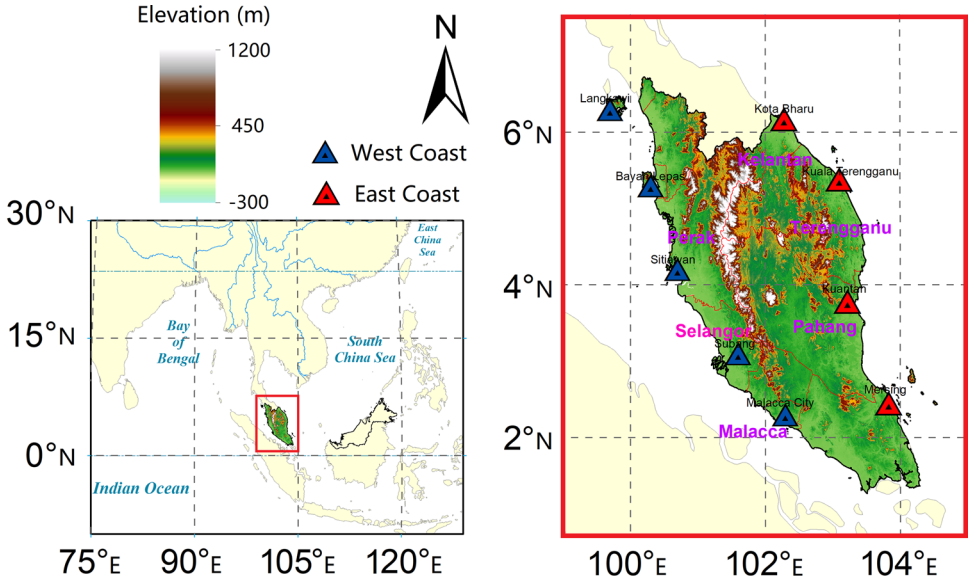

Fig. 1 Location (**a**) and distribution of elevation [**b**, unit: m; data from the 3 arc-seconds elevation data of the Shuttle Radar Topography Mission (Farr et al. 2007)] of the study area. The blue (red) triangles denote the locations for the west (east) coast stations as per our analysis of the precipitation annual cycle. States affected by the extreme flood event during the winter of 2021/22 (IFRC 2021) are labelled in purple

CHIRPS. The Hh-Hv simulations exhibit the best performance in simulating the precipitation distribution during the northeast monsoon season (NDJF) in terms of the centered root-mean-square deviation (RMSD), as shown in Fig. 2c. It also best represents the observed high precipitation amount (> 800 mm per season) along the east coast and west coast as shown in Figure S1. The Lh-Hv is the second best-performing ensemble and it presents the highest correlations with the observed pattern. Similar results are found for the extreme precipitation rate (Fig. 2e). For the southwest monsoon season (MJJA), the Lh-Hv simulations show the lowest RMSD, implying the best performance out of all the ensemble groups. Other ensembles with increased resolution exhibit no apparent improvements, such as the Hh-Hv simulations which capture a local maximum precipitation amount that is to the east of the observed peak (Fig. S2). Additionally, for extreme precipitation during the MJJA periods, the Hh-Hv and Lh-Hv simulations outperform the other two resolution groups, which implies the importance of using fine vertical resolution to improve the simulation of extreme precipitation. Such improved extreme precipitation simulations have also been reported by Volosciuk et al. (2015) with a GCM simulation at an increased vertical resolution. Volosciuk et al. (2015) also suggested that a sufficiently high vertical resolution is important for a GCM to correctly simulate the meridional distribution of extreme precipitation near the tropics.

In summary, GCMs with higher horizontal and vertical resolutions exhibit a better representation of precipitation distribution over Peninsular Malaysia during the northeast monsoon season, while such an improvement is not apparent for the precipitation accumulated during the southwest monsoon season.

3.2 Projected changes in monsoon season precipitation

3.2.1 Northeast monsoon season

During the northeast monsoon season (NDJF, Fig. 3), all the model ensembles except Lh-Lv project a decrease in precipitation (by − 5 to − 11%) over the northeast coast and southeast coast of Peninsular Malaysia. The largest relative decreases are seen in the Lh-Hv simulations (Fig. 3f). However, such projected decreases in precipitation are only statistically significant (p value < 0.05, based on the Student's t test) for the simulations with increased horizontal resolutions, including Hh (Fig. 3b), Hh-Lv (Fig. 3g) and Hh-Hv (Fig. 3h). The simulations with increased model resolutions, including Hh and Hv (Fig. 3d) project more pronounced decreases in precipitation than Lh (Fig. 3a) and Lv (Fig. 3c). A statistically non-significant increase (p value > 0.1) is seen over the western part of the region for all the resolution groups except Lh-Hv. Comparing the spatial pattern of the projected precipitation changes with the mean precipitation patterns during the baseline period (Fig. S1), the projected precipitation decreases in the observed local maximum precipitation along the east coast and the increases over the relatively dry area in the west imply a more evenly distributed seasonal precipitation in the near future.

To quantify the detectability of projected changes in NDJF precipitation in this region from the multi-model GCM ensembles of different resolution groups, the distribution of SNR for the projected changes in each group is displayed in Fig. 4. Compared with Lh (Fig. 4a), the SNR values for the Hh simulations (Fig. 4b) are generally greater, especially for the southeast coastal area near Mersing of

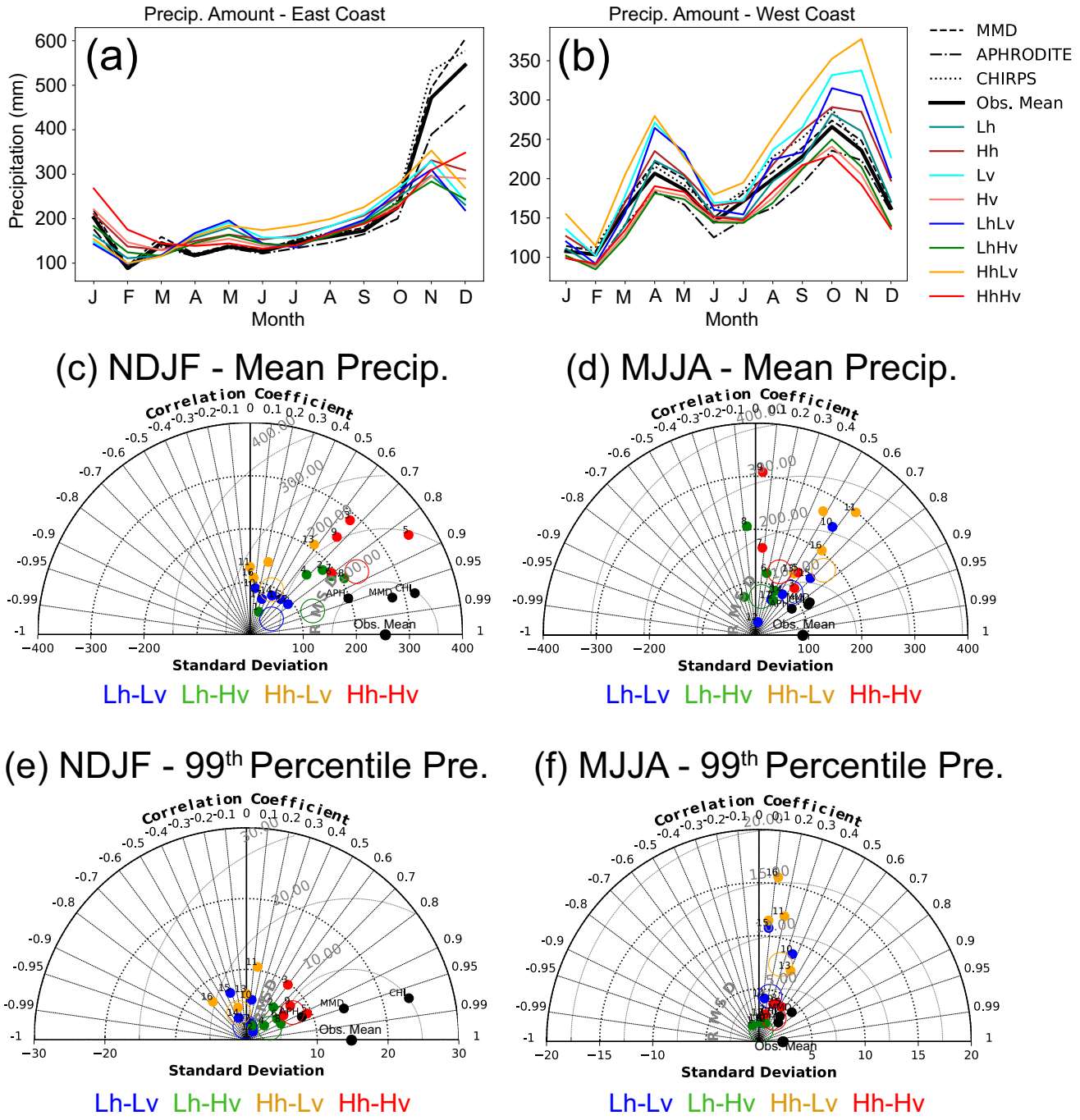

Fig. 2 Baseline evaluations for the period 1981–2000 in terms of temporal (annual cycle) and spatial analyses of precipitation for the multi-GCM ensemble mean of different resolution classes compared with three precipitation observation datasets: **a** annual cycle along the east coast; **b** annual cycle along the west coast; **c**, **d** show Taylor diagrams for the spatial comparisons of the precipitation amount during the northeast and southeast monsoon seasons respectively between the ensemble mean of observed precipitation and each simulation for the different resolution classes; **e**, **f** are as **c**, **d** but for the 95th percentile daily precipitation rate

eastern Johor where a significant decrease in precipitation is projected (Fig. 3b). This implies that the projected change in this area is more notable in ensembles with increased horizontal resolutions. A similar result is seen when comparing Hv (Fig. 4d) with Lv (Fig. 4c). In addition, the SNR values for Lh-Hv (Fig. 4f) and Hh-Hv (Fig. 4h) are generally greater than Lh-Lv (Fig. 4e) and Hh-Lv (Fig. 4g), suggesting that the sensitivity of SNR to the increase in vertical resolution is higher than that to horizontal resolution. This can be partly explained by the general reduction in the

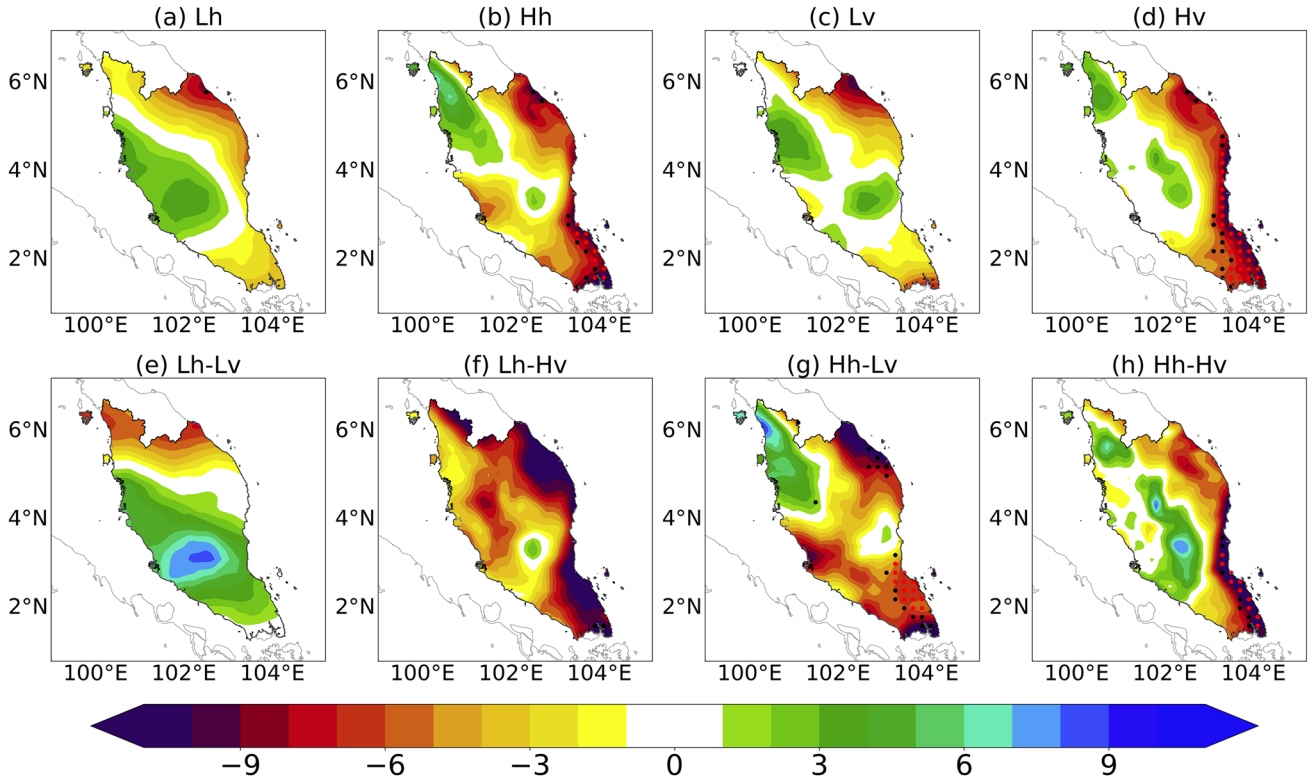

Fig. 3 Relative changes (%) in precipitation during the northeast monsoon season (November to February, NDJF) for the period 2031–2050 relative to the baseline period (1981–2000). Stippling indicates the changes that are statistically significant at a confidence level above 90% (black, two-tailed p value < 0.1) or 95% (red, p value < 0.05) based on Student's t test

ensemble spread over the north and Kuantan for simulations with increased vertical resolutions (Hv, Lv-Hv and Hh-Hv) compared to Lv, Lh-Lv and Hh-Lv (Fig. S3).

3.2.2 Southwest monsoon season

Figure 5 shows the projected changes in precipitation during the southeast monsoon season (MJJA). All the GCM ensembles project a general increase in seasonal precipitation (by up to 12–33%) and the greatest magnitude of the projected changes tends to be within the northwest of the region (e.g., Perak). It is noted that the increase in horizontal resolution results in larger magnitudes of changes when comparing Lh (Fig. 5a) with Hh (Fig. 5b). In addition, the magnitude of the projected changes in Hh-Lv (Fig. 5g) is generally higher, while the projected changes are not statistically significant (p value > 0.1), in contrast to other resolution groups. The Hh-Hv (Fig. 5h) simulations indicate a statistically significant increase in precipitation over the north (p value < 0.05), while the area with significant increases is less widespread than the projected increases with lower horizontal resolutions, including Lh-Lv (Fig. 5e) and Lh-Hv (Fig. 5f).

For the analyses of SNR, the values during MJJA (Fig. 6) are generally greater than those in NDJF (Fig. 4), which is partially due to the generally lower ensemble spreads as shown by Fig. S4 compared to Fig. S3. However, the ensembles at relatively high model resolutions, i.e., Hh (Fig. 6b) and Hv (Fig. 6d), exhibit a smaller SNR than those at lower model resolutions (Fig. 6a, c). Although the Hv simulations (Figure S4d) exhibit a smaller ensemble spread compared to Lv (Fig. S4c), the increase in model resolution is generally not effective in increasing SNR during MJJA.

In summary, the HighResMIP experiments examined in this paper project a general increase in precipitation over Peninsular Malaysia during the southwest monsoon season (MJJA), in contrast to the decrease projected during the northeast monsoon season (NDJF). Additionally, increases in model resolutions, particularly vertical resolution, provide a more certain near-future projection during NDJF by reducing the ensemble spread and increasing SNR of the projected changes, while such effects are not apparent during MJJA. Note that the improvement in the historical precipitation simulation by increasing model resolutions is more pronounced in NDJF than that in MJJA (Fig. 2c–f), which may correspond with the contrasting SNR changes for different seasons. However, although the decreased MME biases imply a higher reliability of the performance, it cannot directly relate to the decreased uncertainties in the future

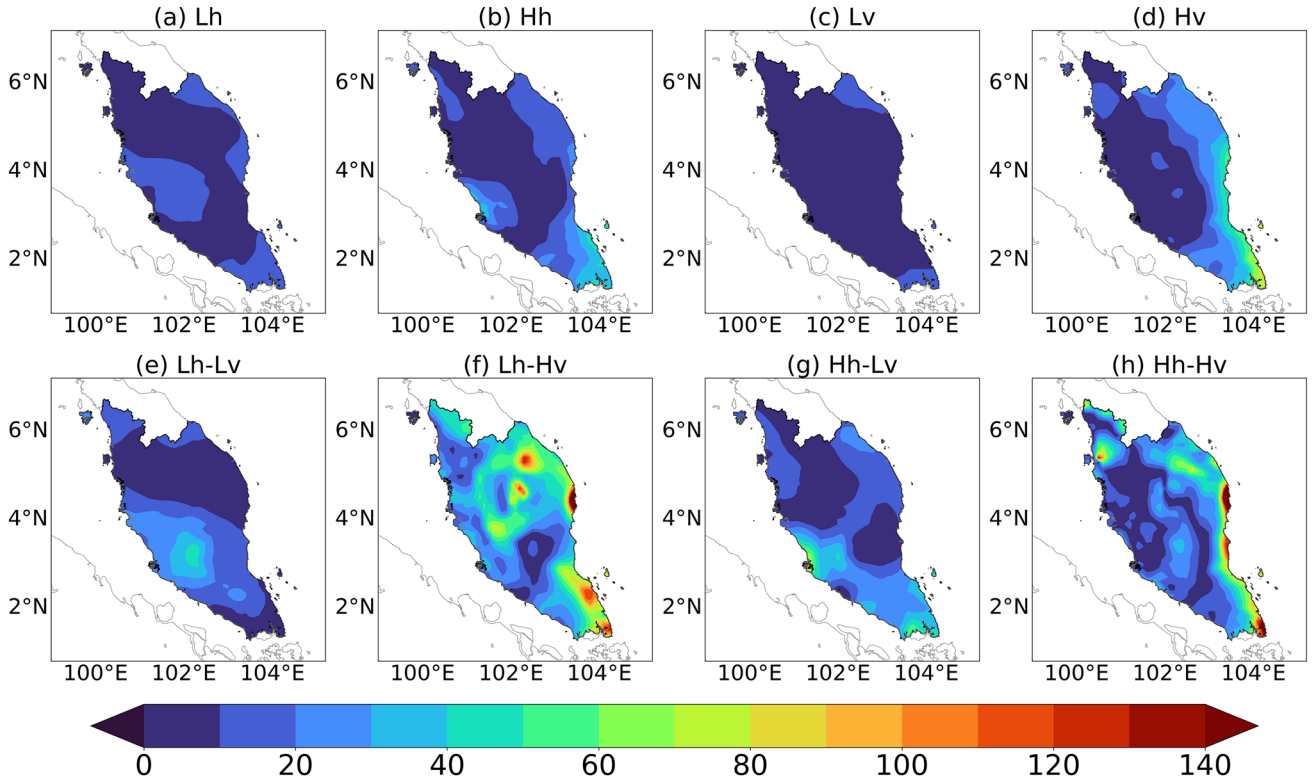

Fig. 4 Signal-to-noise ratios (%) in terms of the projected relative changes divided by the ensemble spread during the northeast monsoon season for the period 2031–2050 relative to the baseline period (1981–2000)

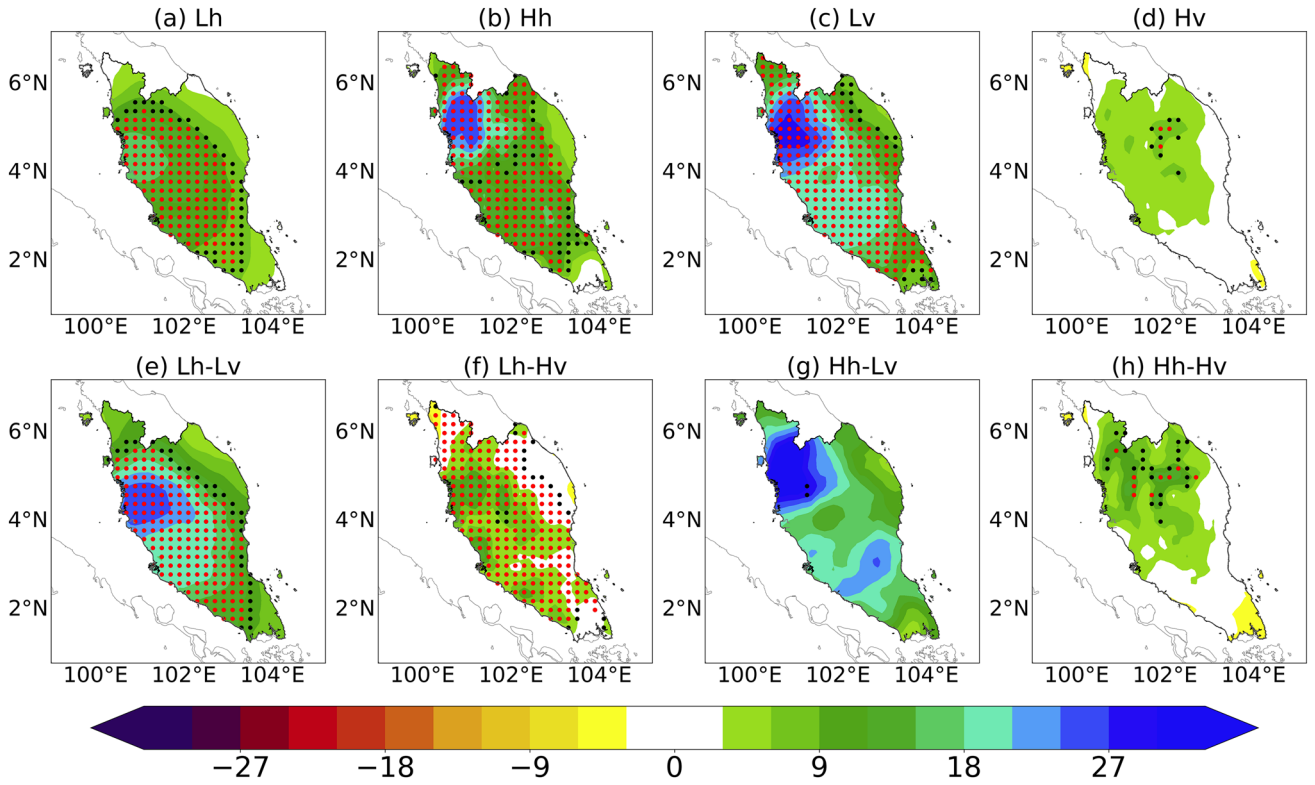

Fig. 5 As Fig. 3, but for the relative changes during the southwest monsoon season from May to August (MJJA)

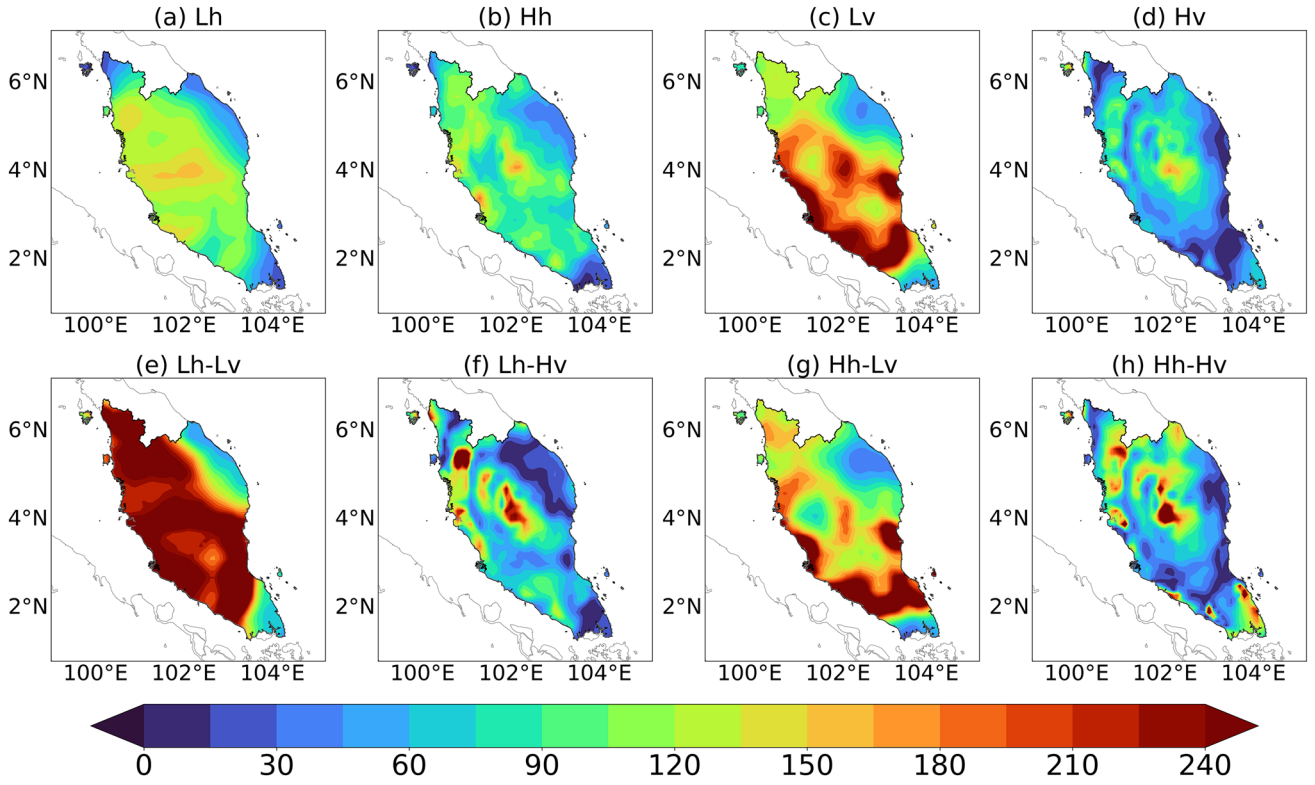

Fig. 6 As Fig. 4, but for the southwest monsoon season from May to August (MJJA)

projection of precipitation with lower ensemble spreads and higher SNR. Hence, further research is needed to clarify the potential link between model biases and future projection uncertainties.

3.3 Changes to the precipitation annual cycle

Figure 7 shows the projected changes in monthly mean precipitation averaged over the east and west coasts of Peninsular Malaysia. Along the east coast, the ensembles of Lh, Hh, Lv and Hv project a significant decrease (by about 10–23%) in precipitation for January (Fig. 7a). Ensembles with lower resolutions, i.e., Lh and Lv, show a significant increase (by about 8–20%) during July to August, while such an increase is less significant in Hh and Hv. Similar changes are projected by Lh-Lv, Lh-Hv, Hh-Lv and Hh-Hv (Fig. 7b); however, only the Lh-Hv simulations exhibit statistically significant changes in January, May and July. No significant change is observed for Hh-Lv.

Along the west coast, Lh, Hh, Lv and Hv project a significant increase in precipitation (by about 17–32%) in July and August (Fig. 7c). For the Lv simulations, significant increases are seen in the early northwest monsoon season (October–November) and a significant decrease is found in January. Similar results are seen for Lh, Hh and Lv, though the projected changes are generally not statistically significant. For the comparison among Lh-Lv, Lh-Hv, Hh-Lv and Hh-Hv (Fig. 7d), the Lh-Hv simulations show the most pronounced increase during the southwest monsoon season (by up to 46% in August) and a significant decrease in the late northwest monsoon season (by about 18% in January). Lh-Lv projects similar changes to Lh-Hv while the statistically significant changes only appear in July and August. For Hh-Hv, the models project a significant increase (by about 22%) in July. No significant change is found for Hh-Lv.

In summary, the selected HighResMIP experiments project an increase in precipitation during the mid-late southwest monsoon season (July to August). Some signals of the projected decreases (increases) in precipitation are noted during the late (early) northeast monsoon season, though the magnitudes of these changes are less pronounced than those projected in the southwest monsoon season. These changes imply that the seasonality of precipitation in the coastal regions of Peninsular Malaysia may weaken in the near future.

3.4 Changes to extreme precipitation

Previous precipitation studies over Peninsular Malaysia have revealed that the occurrence of extreme precipitation during the northeast monsoon season can trigger severe floods across the east coast (e.g. Tangang et al. 2008; Hai et al.

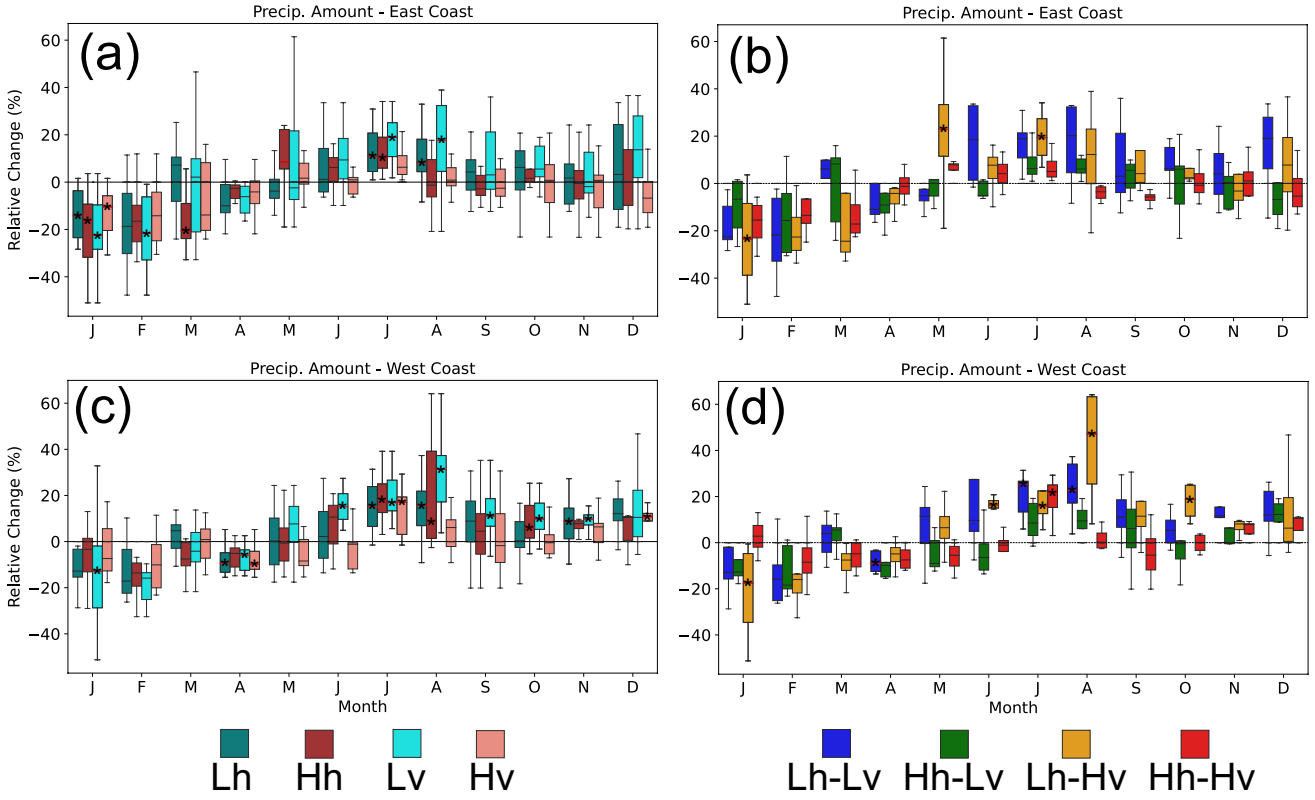

Fig. 7 Projected relative changes in monthly mean precipitation along the east coast (**a**, **b**) and west coast (**c**, **d**) for the period 2031–2050 relative to the baseline period (1981–2000) in ensembles of different resolution classes. Asterisks show the medians of changes that are statistically significant at confidence levels above 90% (two-tailed p value < 0.1, based on Student's t test)

2017); hence, it is important to understand the possible future changes in extreme precipitation in this region. In this section, the projected changes in extreme precipitation rate, in terms of the 95th percentile daily precipitation of the season, by the mid-21st century under the SSP5-8.5 scenario are analyzed for both the northeast monsoon season (NDJF) and the southwest monsoon season (MJJA). Although the extreme precipitation in MJJA is less frequent and weaker than that in NDJF as observed by Syafrina et al. (2015) as well as in Figures S5 and S6, its future projection is reported here due to the pronounced impact of extreme precipitation on the western part of the peninsula during the southwest monsoon season. It is also important to understand its projected changes given the significant projected increases in precipitation for MJJA discussed in the earlier sections.

During the northeast monsoon season (Fig. 8), all the model ensembles project a general increase in extreme precipitation rate over most of the peninsula. These increases exhibit greater statistical significance than those of the projected changes in total precipitation accumulation as shown in Fig. 3. The largest magnitude of increase (by up to about 30%) is found over the south of the region for the model ensembles at lower model resolutions, including Lh (Fig. 8a), Lv (Fig. 8c) and Lh-Lv (Fig. 8e); however, the location shifts towards the northwest as shown in simulations with increased model resolutions, including Hh (Fig. 8b), Lv-Hv (Fig. 8f) and Hh-Lv (Fig. 8g). Simulations at increased vertical resolution, including Hv (Fig. 8d), Lh-Hv and Hh-Hv (Fig. 8h), show less pronounced increases compared to those at lower vertical resolutions (Lv, Lh-Lv and Hh-Lv). In addition, Hv and Hh-Hv project a significant decrease (by up to 12%) over the southeast coast. Some decreases are seen over the northeast coast, especially for Hh, Lh-Hv and Hh-Lv, and these changes correspond with the projected decreases in precipitation accumulation (Fig. 3).

For the southwest monsoon season (Fig. 9), all the model ensembles project a general increase in extreme precipitation rate over most of the peninsula. These increases are more statistically significant than those displayed by the projected changes in precipitation accumulation as shown in Fig. 5. The largest magnitude of increase (by up to above 33%) is found over the northwest. The Hh simulations (Fig. 9b) show larger magnitudes of increases than those projected by Lh (Fig. 9a); however, models with increased vertical resolution (Hv, Fig. 9d) lead to smaller magnitude changes compared

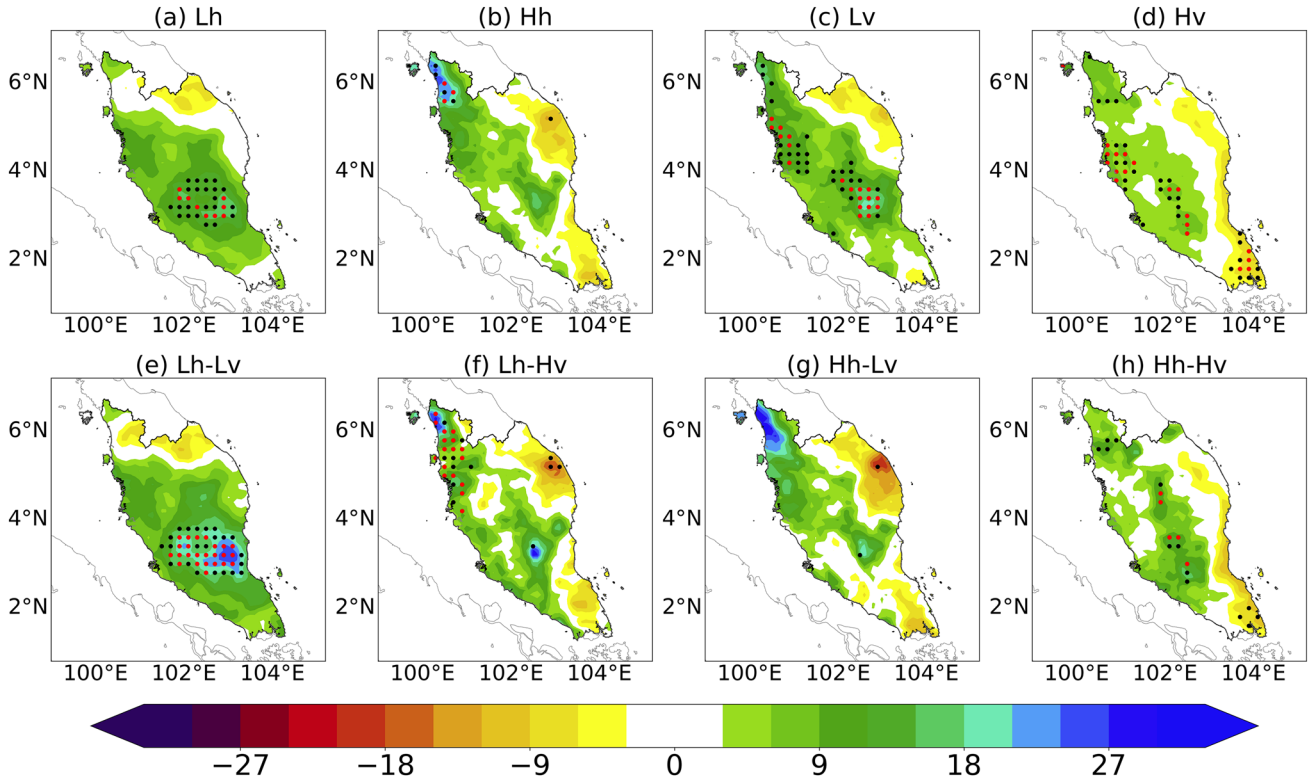

Fig. 8 As Fig. 3, but for the changes in the 95th percentile daily precipitation during the northeast monsoon season (NDJF)

to models at lower vertical resolutions (Lv, Fig. 9c). For the comparison among Lh-Lv, Lh-Hv, Hh-Lv and Hh-Hv (Fig. 9e–h), the Lh-Lv simulations show the most pronounced increases during the southwest monsoon season (by above 33% in most of the western areas). Similar to the projections for seasonal precipitation accumulation (Fig. 5), the projected changes in extreme precipitation by Hh-Lv are not statistically significant (p-value > 0.1). For Hh-Hv, the models project a significant increase (by up to about 15%) over the north, while the magnitudes of change are less pronounced than Lh-Lv and Lh-Hv.

In summary, the selected HighResMIP model experiments project an increase in extreme precipitation, in terms of the 95th percentile daily precipitation rate, during both the northeast and southwest monsoon seasons. The most pronounced increases tend to occur in the northwest of Peninsular Malaysia, while projections for the east coast (where significant increases in the frequency of extreme precipitation events have been observed in recent decades, Khan et al. 2019) are less pronounced than those projected across the west. These changes also indicate a more spatially even distribution of extreme precipitation rates in the near future.

3.5 Relationship between the projected changes in precipitation and large-scale environments

To understand the large-scale physical processes dominating the projected precipitation changes discussed in the previous section, here we analyze the projected changes in precipitation-associated environmental fields for different monsoon seasons under the SSP5-8.5 scenario. This section also provides a brief validation of the simulations for the large-scale fields during the historical baseline period by comparing them to those in the four climate reanalysis datasets listed in Table 2.

3.5.1 Northeast monsoon season

Vectors in Fig. 10 show the mean horizontal moisture transport, in terms of the vertically integrated water vapor transport (IVT), during the northeast monsoon season (NDJF) for the baseline period (1981–2000). The reanalysis datasets (Fig. 10a–d) show the domination of intense southwestward moisture transport by the northeast monsoon flow over Peninsular Malaysia. A cyclonic horizontal wind shear affecting the southeast of the region is observed, which is associated with the counterclockwise turning of the cross-equatorial winds associated with terrain effects (Chang et al. 2016). These large-scale characteristics are correctly simulated

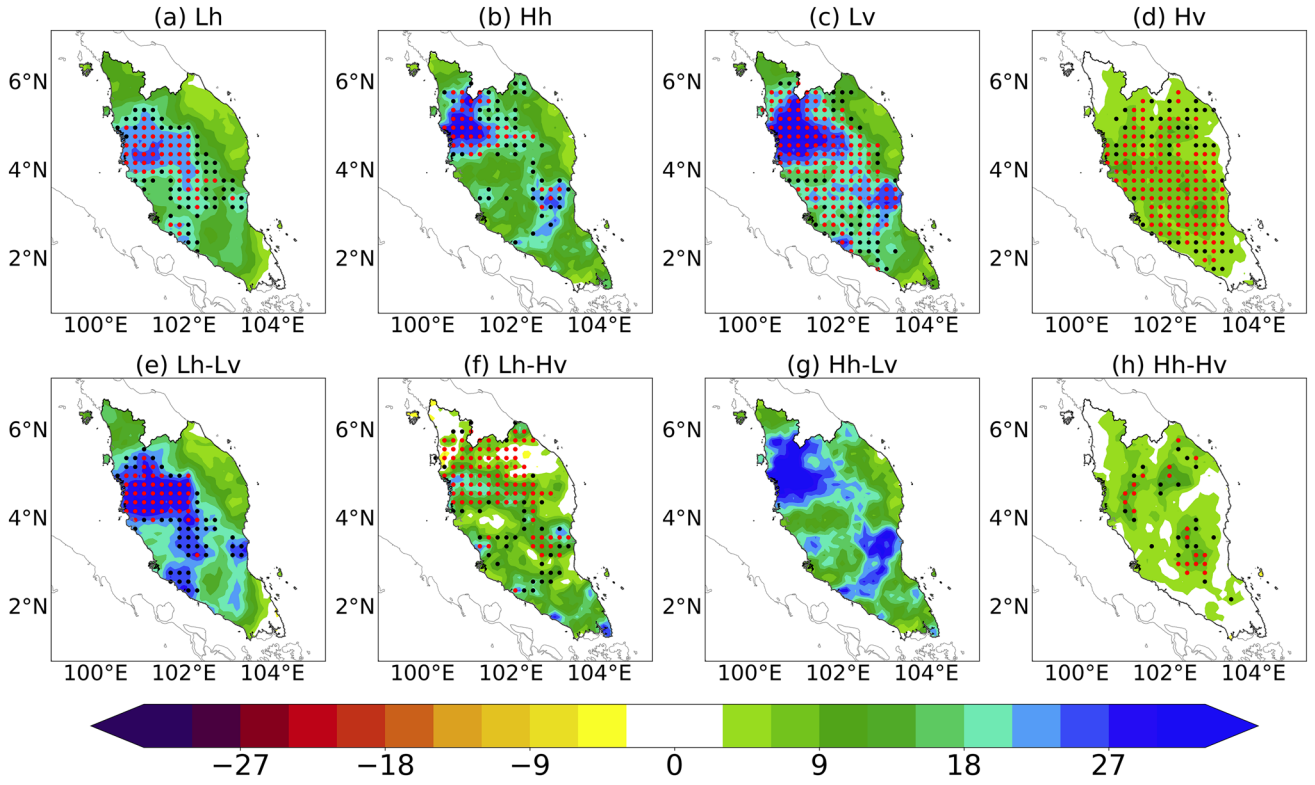

Fig. 9 As Fig. 8, but for the southwest monsoon season (MJJA)

by ensembles of all the model groupings (Fig. 10e–l). The analyses of bias distributions for similar model groups relative to different reanalysis datasets can be found in L2021.

The projected changes (for the future period of 2031–2050 relative to the baseline period of 1981–2000) in the magnitudes of IVT near Peninsular Malaysia by different resolution groups (Fig. 10e–l) show a general weakening (by up to about 20 kg $m^{-1}s^{-1}$ over the southwest of the region) of the southwestward moisture transport by the northeast monsoon in all the model simulations except Lv (Fig. 10g) and Lh-Lv (Fig. 10i). This agrees well with the general decrease in precipitation over the east coast (Fig. 3) due to the weaker orographic precipitation effect (Juneng et al. 2007). It also explains the less substantial precipitation decreases along the east coast projected by Lv (Fig. 3c) and Lh-Lv (Fig. 3e) as compared to other simulations. For the projected weakening of IVT, the changes presented by Hh-Lv (Fig. 10k) are not statistically significant, which partly explains the statistically non-significant changes in extreme precipitation shown in Fig. 8g. A similar relationship between the weakening of the northeast monsoon flow during winter and precipitation decreases over the east coast is also presented by Tangang et al. (2020) for projections under two RCP scenarios from the Coordinated Regional Climate Downscaling Experiment–Southeast Asia (CORDEX–SEA) ensembles.

Due to the close relationship between the temporal and spatial changes in precipitation near Malaysia and changes in the atmospheric ascent associated with topographic forcing (Mahmud et al. 2020) and different climate regimes (Salimun et al. 2014), we discuss the projected changes in vertical velocity fields at 850 hPa by the selected HighResMIP experiments. For simulations during NDJF for the baseline period (1981–2000), the east coast of Peninsular Malaysia is dominated by relatively strong vertical ascent (up to $6–15 \times 10^{-2}$ Pa s^{-1}), as evidenced by the four reanalysis datasets (Fig. 11a–d). Such a distribution is reasonably represented by the selected model simulations (Fig. 11e–l); however, simulations at relatively low resolutions [Lh (Fig. 11e), Lv (Fig. 11g) and Lh-Lv (Fig. 11i)] simulate an ascent of up to $6–9 \times 10^{-2}$ Pa s^{-1} along the east coast, which is weaker than those in simulations with increased resolutions [Hh (Fig. 11f), Hv (Fig. 11h), Hh-Lv (Fig. 11k) and Hh-Hv (Fig. 11L)]. The magnitude of ascent (up to 15×10^{-2} Pa s^{-1}) captured by the Hh-Hv simulations are most similar to those in ERA5 and CFSR.

For the future period (2031–2050) relative to the baseline period, all the model groupings project a significant weakening (p value < 0.05) of the vertical ascent (up to $0.9–2.1 \times 10^{-2}$ Pa s^{-1}) along the east coast (Fig. 11e–l) associated with the general weakening of the monsoon flow (Fig. 10e–l). Also, the models tend to project a

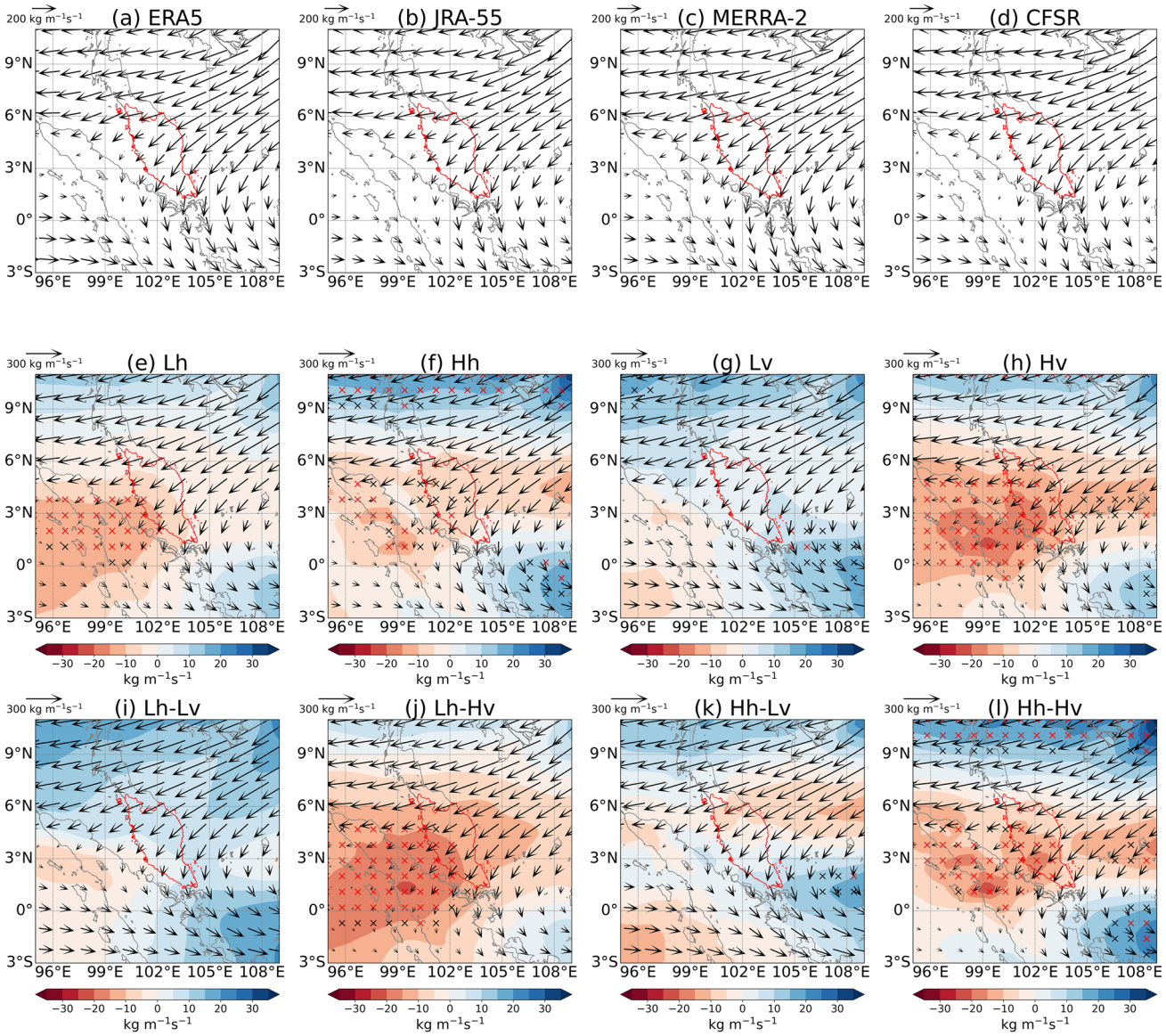

Fig. 10 NDJF-mean fields of the vertically integrated water vapor transport (IVT, vectors) for the baseline period (1981–2000) and their projected absolute magnitude changes (shaded in e–l) for the period 2031–2050 relative to the baseline period in each resolution class. Cross symbols denote the changes that are statistically significant at a confidence level above 90% (black, two-tailed p value < 0.1) or 95% (red, p value < 0.05) based on Student's t test. Simulations from NICAM16 and HiRAM-SIT are not included in these analyses due to the lack of relevant data

non-significant (p value > 0.1) increase in vertical ascent by up to 0.3–2.1 $\times 10^{-2}$ Pa s^{-1} over the west of the peninsula. Such a change is consistent with the more evenly distributed precipitation (Fig. 3) and the extreme precipitation rates (Fig. 8) with decreased (increased) signals over the east (west). Simulations with increased horizontal resolutions (Hh) tend to exhibit a larger magnitude of changes compared to those with lower horizontal resolutions (Lh). Similar differences in projected changes are observed when comparing Hv with Lv. These are generally consistent with the differences in projected precipitation changes shown in Fig. 3a–d.

3.5.2 Southwest monsoon season

For the southwest monsoon season (MJJA) during the baseline period (1981–2000), the IVT fields from four reanalyses (Fig. 12a–d) show that Peninsular Malaysia, especially for the northern area, is dominated by the southwesterly moisture transport. The cross-equatorial southeasterly flow dominates the areas to the south, which can induce

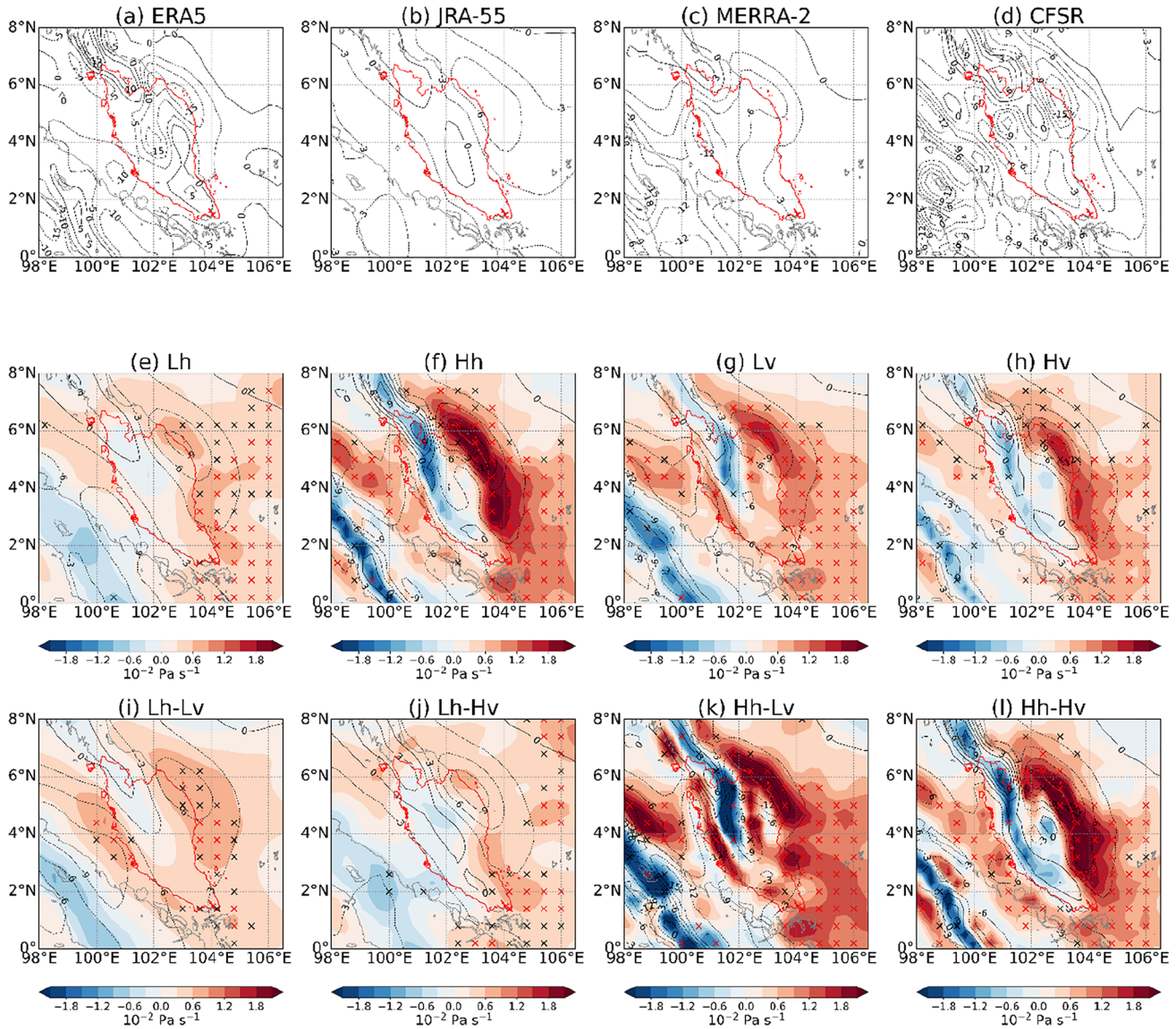

Fig. 11 As Fig. 12 but for the NDJF-mean fields of vertical velocity at 850 hPa (positive: downward motion) for the baseline period from 1981 to 2000 (black contours) and their projected changes for the period 2031–2050 (shaded) relative to the baseline period

low-level moisture convergence over the peninsula (Chang et al. 2016). In addition, the relatively strong westerly flow to the north can lead to strong anti-cyclonic shear over the peninsula, which is closely associated with reduced convection and the associated precipitation reduction of the season (Chenoli et al. 2018). These large-scale characteristics are correctly represented by all the resolution groups (Fig. 12e–l). For projected changes during 2031–2050 relative to the baseline, all the resolution groups project a weakening (by up to 35 kg $m^{-1}s^{-1}$) of the moisture transport by the southwest monsoon flow to the north of the peninsula, implying a weakening of the anticyclonic shear dominating the region in summer. In addition, a strengthening of the cross-equatorial southeasterly is observed to the south (by up to 30 kg $m^{-1}s^{-1}$). These changes create a more favorable environment for precipitation over the peninsula, which corresponds well with the general increase in precipitation and extreme precipitation rates as shown in Figs. 5 and 9. Comparing the different resolution groups, the Hh (Fig. 12f) simulations project a more significant strengthening (p value < 0.05) of the cross-equatorial southeasterly flow than Lh (p value > 0.05, Fig. 12e), while Hv (Fig. 12h) projects a less pronounced strengthening compared to Lv (Fig. 12g). These changes are consistent with the magnitude of increases in precipitation (Fig. 5a–d) and extreme precipitation rates (Fig. 9a–d). For the southwest monsoon flow to the north of 6°N, the projected weakening by Hv (p value < 0.05) is more

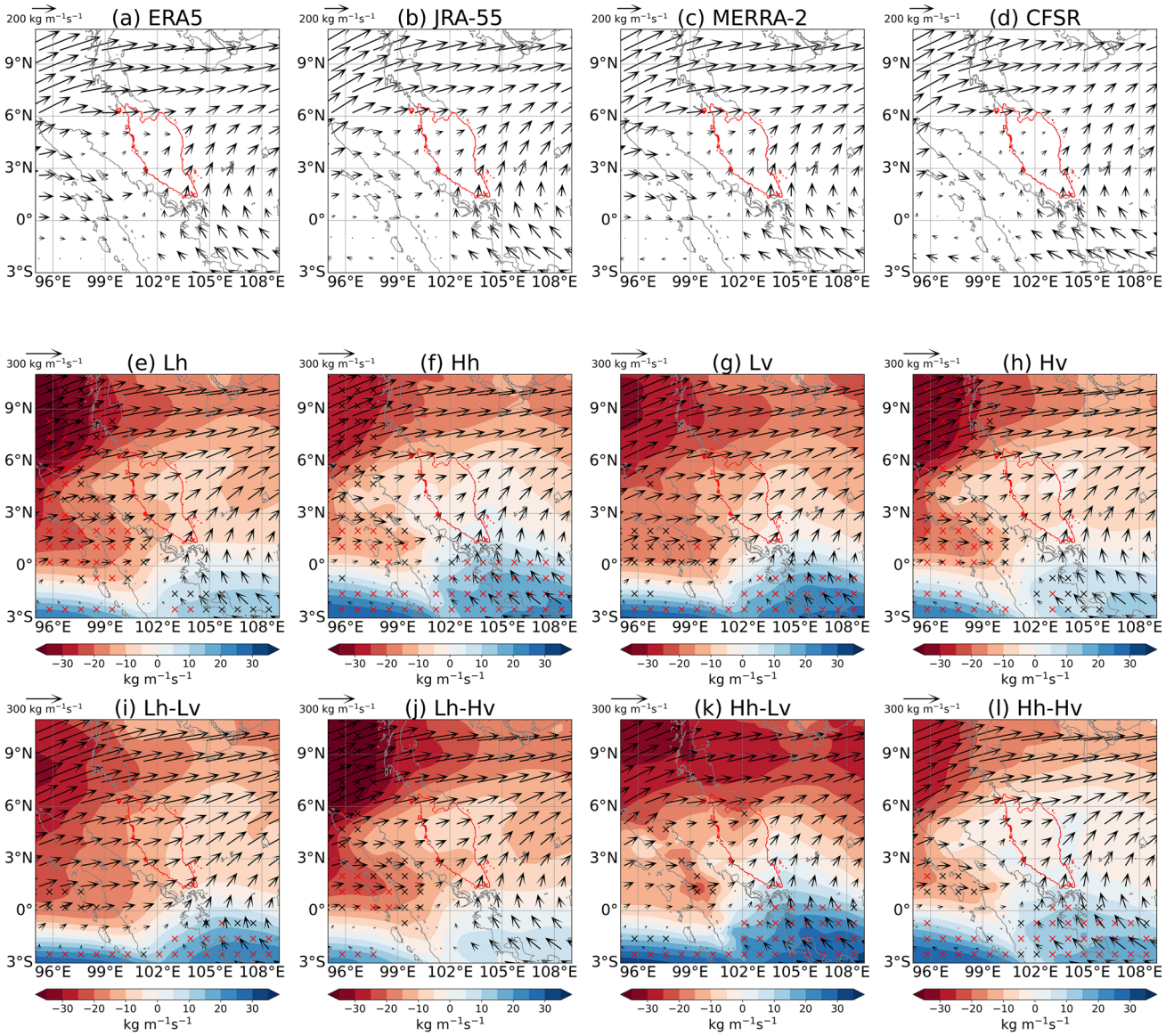

Fig. 12 Same as Fig. 10, but for the MJJA-mean fields

pronounced than other resolution groups. However, these changes are difficult to reconcile with the less pronounced increase in precipitation for Hv (Fig. 5d) compared to Lv (Fig. 5c). For the comparison among Lh-Lv, Lh-Hv, Hh-Lv and Hh-Hv, the Hh-Lv simulations (Fig. 12k) project the greatest enhancement of the cross-equatorial southeasterly flow. This is consistent with the largest magnitude of precipitation increase over the northwest projected by Hh-Lv (Fig. 5g).

Figure 13 shows the analysis of vertical velocity at 850-hPa during MJJA. The four reanalysis datasets show a relatively strong vertical ascent (up to 3–20×10^{-2} Pa s^{-1}) across the mid-north of Peninsular Malaysia for the baseline period (Fig. 13a–d), which may be related to the low-level convergence between the cross-equatorial southwesterly flow to the south of the region and the westerly monsoonal flow from the north of Sumatra. All the model groupings (Fig. 15e–l), except Hh–Lv (Fig. 15k), underestimate the vertical ascent in the middle of the peninsula compared to ERA5, JRA-55 and CFSR. For the projected future changes, all the model groupings project a strengthening (up to a range of 0.9–2.1×10^{-2} Pa s^{-1}) of the vertical ascent over the north of the peninsula, which can be related to the location of the greatest magnitudes of precipitation increase projected by all the groups (Figs. 5, 9). Such strengthening is only statistically significant (p value <0.05) in Lv (Fig. 13g) and Hh-Lv (Fig. 13k), which explains the more pronounced

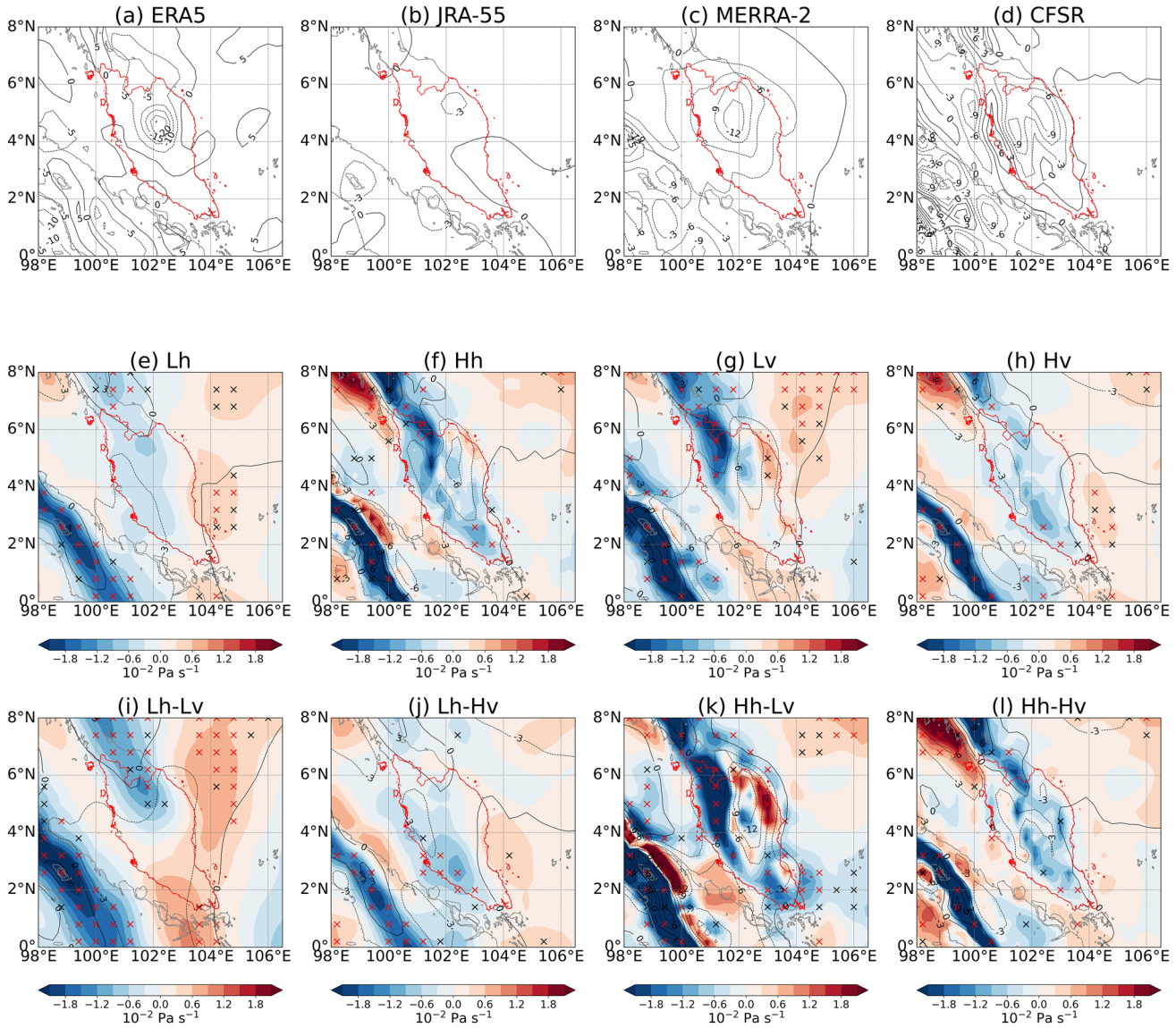

Fig. 13 Same as Fig. 11, but for the MJJA-mean fields

precipitation increases in these simulations compared to other resolution groups.

In summary, the projected changes in the precipitation-related environmental fields generally agree well with the projected changes in precipitation and the extreme precipitation rates over Peninsular Malaysia. These include the weakening of the moisture transports by the monsoonal flow in different monsoon seasons, which partly explain the weaker seasonality of precipitation in the coastal regions as well as the more evenly distributed precipitation in NDJF and the precipitation increase in MJJA. Moreover, the changes in the vertical velocity in the lower troposphere for different seasons are partially consistent with the distributions of the projected precipitation changes. However, some projected signals are difficult to relate to the large-scale environmental changes. For instance, although the more pronounced changes in the large-scale environments projected by the Hh-Lv simulations agree with the relatively large magnitudes of their projected precipitation changes, it is difficult to explain why the precipitation changes in Hh-Lv are generally not statistically significant given the robustness of changes in the environmental fields examined here.

4 Summary and discussion

In this paper, the ability of eighteen selected CMIP6 HighResMIP experiments to simulate the monsoon season precipitation for the historical period of 1981–2000

has been evaluated as an extension of the recent study of L2021 that focused on the period 2001–2014. Based on the evaluated GCMs and their future climate simulations under the SSP5-8.5 scenario, the projected near-term changes in monsoon precipitation have been presented for the future period (2031–2050) relative to the historical period (1981–2000). Our primary findings are summarized as follows:

1. The selected HighResMIP experiments project a decrease in precipitation over Peninsular Malaysia during the northeast monsoon season (NDJF), especially along the east coast of the region. For the southwest monsoon season (MJJA), a general increase in precipitation is found near the northwest of the region. These changes imply that both the spatial and temporal distributions of precipitation in Peninsular Malaysia may become more evenly spread.
2. Both horizontal and vertical model resolutions play an important role in the projected signals. For instance, the projected decreases in NDJF precipitation along the east coast are found to be more significant in simulations with increased horizontal and vertical resolutions. For MJJA, simulations with increased vertical resolutions tend to project smaller magnitudes of precipitation increases.
3. Simulations with increased horizontal and vertical resolutions exhibit some potential to narrow uncertainty in the future projection of precipitation during the northeast monsoon season: Greater SNR values for the projected precipitation changes during NDJF have been found in simulations with increased horizontal and vertical resolutions. For the southwest monsoon season (MJJA), the increase in model resolution shows no apparent effect on enhancing the SNR. It is difficult to understand the cause of such different resolution-dependance on projection uncertainties in different seasons, which requires future studies.
4. The projected decrease in precipitation along the east coast during NDJF can be related to the weakening of the northeast monsoon flow and the associated weakening of the low-level ascent. For MJJA, the general increase in precipitation and extreme precipitation rates over the peninsula can be explained by the increased vertical ascent over the peninsula, associated with the weakening of the low-level anticyclonic shear and a strengthening of the cross-equatorial southeasterly flow to the south.

The projected results highlighted in this paper show some consistency with previous studies focusing on Peninsular Malaysia or the wider Southeast Asia region. For example, using an ensemble of regional climate model simulations under the RCP4.5 and 8.5 scenarios, Tangang et al. (2020) projected an increase in the seasonal maximum of daily precipitation over the north of Peninsular Malaysia in summer and over the west in winter by the end of 21st century, which is consistent with the projected increases in the 95th percentile daily precipitation in this study. Based on multiple GCMs, the studies of Sun and Ding (2010) and Zou and Zhou (2015) projected a weakening of the southwest summer monsoon flow over Southeast Asia under the RCP 8.5 scenario, which agrees well with the projected changes in MJJA IVT in this paper. The projected weakening of the winter monsoon in Southeast Asia has also been reported by Tangang et al. (2019) based on the CORDEX-SEA ensemble and by Siew et al. (2014) based on the CMIP5 coupled experiments. The projected increases in extreme precipitation rates over Peninsular Malaysia for both the monsoon seasons demonstrate some similarities to the projected increases in different levels of annual extreme precipitation rates over Thailand based on the HighResMIP simulations for the same emission scenario (Khadka et al. 2021). In contrast, a projected strengthening of the summer and winter monsoonal flows near Southeast Asia has also been found by Dai et al. (2021) based on the CMIP5 simulations under the RCP4.5 scenario. These contrasting results imply uncertainties in the future projection of monsoon circulation that requires further attention in future studies.

This paper has evaluated the role of model spatial resolution in projected changes in precipitation over Peninsular Malaysia in a set of state-of-the-art GCMs. Such a resolution dependence can strongly influence the result of watershed-scale hydrological modeling driven by the GCM simulations (Tan et al. 2021). However, this impact has not been thoroughly investigated, especially the role of vertical resolution, since previous research has typically focused on the effect of improving horizontal resolution. In addition, the results show that increases in both horizontal and vertical resolution can improve the SNR of the projected precipitation changes for the northeast monsoon season. However, the analyses of uncertainties in terms of ensemble spread and SNR are strongly constrained by the available ensemble size, especially for the high-resolution experiments that are computationally expensive. Another limitation of the study is the chosen study periods, limited by the availability of future climate simulation outputs from HighResMIP, which makes it difficult to generalize the effect of long-term climate sensitivity to the anthropogenic greenhouse gas emissions. These limitations are expected to be addressed in future work.

Supplementary Information The online version contains supplementary material available at https://doi.org/10.1007/s00382-022-06363-5.

Acknowledgements The authors acknowledge the European Centre for Medium-Range Weather Forecasts, The Japan Meteorological Agency, The National Aeronautics and Space Administration and The National Centers for Environmental Prediction for providing the climate reanalysis datasets used in the study.

Funding This research was supported by the Newton Fund of The Natural Environment Research Council: IMpacts of PRecipitation from Extreme StormS - Malaysia (IMPRESS-Malaysia, grant number: NE/S002707/1), and Ministry of Higher Education Malaysia (Grant Number: NEWTON/1/2018/SS07/USM//1; 203.PHUMANITI.6780001).

Data availability The used CMIP6 HighResMIP data are downloaded from the data node website of the Lawrence Livermore National Laboratory (https://esgf-node.llnl.gov/projects/cmip6/). The APHRODITE data is downloaded from its official website managed by the Research Institute for Humanity and Nature (http://aphrodite.st.hirosaki-u.ac.jp). The CHIRPS rainfall estimates from rain gauge and satellite observations are downloaded from its official website managed by the University of California, Santa Barbara (https://chc.ucsb.edu/data/chirps). The data generated and analyzed during the current study are available from the corresponding author on reasonable request.

Declarations

Conflict of interest The authors declare that they have no conflict of interest.

References

Amin MZM, Islam T, Ishak AM (2014) Downscaling and projection of precipitation from general circulation model predictors in an equatorial climate region by the automated regression-based statistical method. Theor Appl Climatol 118:347–364. https://doi.org/10.1007/s00704-013-1062-2

Amirabadizadeh M, Ghazali AH, Huang YF, Wayayok A (2016) Downscaling daily precipitation and temperatures over the Langat River Basin in Malaysia: a comparison of two statistical downscaling approaches. Int J Water Resour Environ Eng 8:120–136. https://doi.org/10.5897/IJWREE2016.0585

Anstey JA, Davini P, Gray LJ et al (2013) Multi-model analysis of Northern Hemisphere winter blocking: model biases and the role of resolution. J Geophys Res Atmos 118:3956–3971. https://doi.org/10.1002/jgrd.50231

Chan NW, Parker DJ (1996) Response to dynamic flood hazard factors in Peninsular Malaysia. Geogr J 162:313. https://doi.org/10.2307/3059653

Chang CP, Harr PA, Chen HJ (2005) Synoptic disturbances over the equatorial South China Sea and western maritime continent during boreal winter. Mon Weather Rev 133:489–503. https://doi.org/10.1175/MWR-2868.1

Chang C-P, Lu M-M, Lim H (2016) Monsoon convection in the Maritime Continent: Interaction of large-scale motion and complex terrain. Meteorol Monogr 56:6.1-6.29. https://doi.org/10.1175/amsmonographs-d-15-0011.1

Chenoli SN, Jayakrishnan PR, Samah AA et al (2018) Southwest monsoon onset dates over Malaysia and associated climatological characteristics. J Atmos Sol Terr Phys 179:81–93. https://doi.org/10.1016/j.jastp.2018.06.017

Chin KS, Tan KW (2018) Evaluation of SRE scenarios for Penang, Selangor and Johor in Peninsular Malaysia using PRECIS Regional Climate Model (RCM). In: E3S web of conferences. EDP Sciences, p 05020

Dai X, Yang Y, Wang P (2021) Asian monsoon projection with a new large-scale monsoon definition. Theor Appl Climatol. https://doi.org/10.1007/s00704-021-03866-9

Daud W (2010) Quality control for unmanned meteorological stations in Malaysian Meteorological Department

Endo H, Kitoh A, Ose T et al (2012) Future changes and uncertainties in Asian precipitation simulated by multiphysics and multi-sea surface temperature ensemble experiments with high-resolution Meteorological Research Institute atmospheric general circulation models (MRI-AGCMs). J Geophys Res Atmos 117:1–17. https://doi.org/10.1029/2012JD017874

Eyring V, Bony S, Meehl GA et al (2016) Overview of the Coupled Model Intercomparison Project Phase 6 (CMIP6) experimental design and organization. Geosci Model Dev 9:1937–1958. https://doi.org/10.5194/gmd-9-1937-2016

Farr TG, Rosen PA, Caro E et al (2007) The shuttle radar topography mission. Rev Geophys 45:1–33. https://doi.org/10.1029/2005RG000183

Ge F, Zhu S, Luo H et al (2021) Future changes in precipitation extremes over Southeast Asia: insights from CMIP6 multi-model ensemble. Environ Res Lett 16:024013. https://doi.org/10.1088/1748-9326/abd7ad

Gelaro R, McCarty W, Suárez MJ et al (2017) The modern-era retrospective analysis for research and applications, version 2 (MERRA-2). J Clim 30:5419–5454. https://doi.org/10.1175/JCLI-D-16-0758.1

Gu H, Yu Z, Wang J et al (2015) Assessing CMIP5 general circulation model simulations of precipitation and temperature over China. Int J Climatol 35:2431–2440. https://doi.org/10.1002/joc.4152

Güttler I, Stepanov I, Branković Č et al (2015) Impact of horizontal resolution on precipitation in complex orography simulated by the regional climate model RCA3. Mon Weather Rev 143:3610–3627. https://doi.org/10.1175/MWR-D-14-00302.1

Haarsma RJ, Roberts MJ, Vidale PL et al (2016) High Resolution Model Intercomparison Project (HighResMIP v1.0) for CMIP6. Geosci Model Dev 9:4185–4208. https://doi.org/10.5194/gmd-9-4185-2016

Haarsma R, Acosta M, Bakhshi R et al (2020) HighResMIP versions of EC-Earth: EC-Earth3P and EC-Earth3P-HR—description, model computational performance and basic validation. Geosci Model Dev 13:3507–3527. https://doi.org/10.5194/gmd-13-3507-2020

Hai OS, Samah AA, Chenoli SN et al (2017) Extreme rainstorms that caused devastating flooding across the east coast of Peninsular Malaysia during November and December 2014. Weather Forecast 32:849–872. https://doi.org/10.1175/WAF-D-16-0160.1

Hassan Z, Shamsudin S, Harun S et al (2015) Suitability of ANN applied as a hydrological model coupled with statistical downscaling model: a case study in the northern area of Peninsular

Malaysia. Environ Earth Sci 74:463–477. https://doi.org/10.1007/S12665-015-4054-Y/FIGURES/9
He S, Yang J, Bao Q et al (2019) Fidelity of the observational/reanalysis datasets and global climate models in representation of extreme precipitation in East China. J Clim 32:195–212. https://doi.org/10.1175/JCLI-D-18-0104.1
Hersbach H, Bell B, Berrisford P et al (2020) The ERA5 global reanalysis. Q J R Meteorol Soc 146:1999–2049. https://doi.org/10.1002/qj.3803
Huang D, Yan P, Zhu J et al (2018) Uncertainty of global summer precipitation in the CMIP5 models: a comparison between high-resolution and low-resolution models. Theor Appl Climatol 132:55–69. https://doi.org/10.1007/s00704-017-2078-9
Huffman G, Bolvin DT, Braithwaite D et al (2015) Algorithm theoretical basis document (ATBD) Version 4.5: NASA global precipitation measurement. GPM) Integrated Multi-satellitE Retrievals for GPM (IMERG), Greenbelt
IFRC (2021) Malaysia: flash floods—emergency plan of action (EPoA). https://adore.ifrc.org/Download.aspx?FileId=480596
Inness PM, Slingo JM, Woolnough SJ et al (2001) Organization of tropical convection in a GCM with varying vertical resolution; implications for the simulation of the Madden-Julian oscillation. Clim Dyn 17:777–793. https://doi.org/10.1007/s003820000148
Johnson R, Houze R (1987) Precipitating cloud systems of the Asian monsoon. In: Monsoon meteorology. Oxford University Press, Oxford, pp 298–353
Juneng L, Tangang FT, Reason CJC (2007) Numerical case study of an extreme rainfall event during 9–11 December 2004 over the east coast of Peninsular Malaysia. Meteorol Atmos Phys 98:81–98. https://doi.org/10.1007/s00703-006-0236-1
Juneng L, Tangang FT, Kang H et al (2010) Statistical downscaling forecasts for winter monsoon precipitation in Malaysia using multimodel output variables. J Clim 23:17–27. https://doi.org/10.1175/2009JCLI2873.1
Khadka D, Babel MS, Collins M et al (2021) Projected changes in the near-future mean climate and extreme climate events in northeast Thailand. Int J Climatol 42:2470–2492. https://doi.org/10.1002/joc.7377
Khan N, Pour SH, Shahid S et al (2019) Spatial distribution of secular trends in rainfall indices of Peninsular Malaysia in the presence of long-term persistence. Meteorol Appl 26:655–670. https://doi.org/10.1002/met.1792
Kim IW, Oh J, Woo S, Kripalani RH (2019) Evaluation of precipitation extremes over the Asian domain: observation and modelling studies. Clim Dyn 52:1317–1342. https://doi.org/10.1007/s00382-018-4193-4
Kobayashi S, Ota Y, Harada Y et al (2015) The JRA-55 reanalysis: general specifications and basic characteristics. J Meteorol Soc Japan 93:5–48. https://doi.org/10.2151/jmsj.2015-001
Koseki S, Koh TY, Teo CK (2014) Borneo vortex and mesoscale convective rainfall. Atmos Chem Phys 14:4539–4562. https://doi.org/10.5194/acp-14-4539-2014
Kwan MS, Tangang FT, Juneng L (2014) Present-day regional climate simulation over Malaysia and western Maritime Continent region using PRECIS forced with ERA40 reanalysis. Theor Appl Climatol 115:1–14. https://doi.org/10.1007/S00704-013-0873-5/FIGURES/10
Lee W-K, Mohamad IN (2014) Flood economy appraisal: an overview of the Malaysian scenario. In: InCIEC 2013. Springer, Singapore, pp 263–274
Liang J, Catto JL, Hawcroft M et al (2021) Climatology of borneo vortices in the HadGEM3-GC31 general circulation model. J Clim. https://doi.org/10.1175/jcli-d-20-0604.1
Liang J, Tan ML, Hawcroft M et al (2021) Monsoonal precipitation over Peninsular Malaysia in the CMIP6 HighResMIP experiments: the role of model resolution. Clim Dyn. https://doi.org/10.1007/s00382-021-06033-y
Mahmud MR, Yusof AAM, Reba M, Hashim M (2020) Mapping the daily rainfall over an ungauged tropical micro-watershed: a downscaling algorithm using GPM data. Water (Switzerland) 12:1661. https://doi.org/10.3390/W12061661
Mayowa OO, Pour SH, Shahid S et al (2015) Trends in rainfall and rainfall-related extremes in the east coast of peninsular Malaysia. J Earth Syst Sci 124:1609–1622. https://doi.org/10.1007/S12040-015-0639-9/FIGURES/11
McCrary RR, Randall DA, Stan C (2014) Simulations of the West African monsoon with a superparameterized climate model. Part II: African easterly waves. J Clim 27:8323–8341. https://doi.org/10.1175/JCLI-D-13-00677.1
Mohd MS, Daud D, Alias DB(2006) GIS analysis for flood hazard mapping: case study; Segamat. In: Seminar Nasional GIS: geographic information system application for mitigation in natural disaster. Jakarta, pp 1–15
Muqtada M, Khan A, Ashikin N, Shaari B et al (2014) Flood impact assessment in Kota Bharu, Malaysia: a statistical analysis Faculty of Earth Science, Universiti Malaysia Kelantan, Jeli Campus, School of Quantitative Sciences, Universiti Utara Malaysia. World Appl Sci J 32:626–634. https://doi.org/10.5829/idosi.wasj.2014.32.04.422
Nadrah N, Tukimat A, Harun S (2011) The projection of future rainfall change over Kedah, Malaysia with the statistical downscaling model. Malays J Civ Eng 23:67–79. https://doi.org/10.11113/MJCE.V23N2.269
Nath R, Luo Y (2021) Future projection of extremely hot and precipitation events over Southeast Asian river basins under RCP8.5 scenario. Int J Climatol. https://doi.org/10.1002/JOC.7410
Ngai ST, Sasaki H, Murata A et al (2020) Extreme rainfall projections for malaysia at the end of 21st century using the high resolution non-hydrostatic regional climate model (NHRCM). Sci Online Lett Atmos 16:132–139. https://doi.org/10.2151/SOLA.2020-023
Nguyen-Thuy H, Ngo-Duc T, Trinh-Tuan L et al (2021) Time of emergence of climate signals over Vietnam detected from the CORDEX-SEA experiments. Int J Climatol 41:1599–1618. https://doi.org/10.1002/joc.6897
Noor M, Ismail T, Bin, Ullah S et al (2020) A non-local model output statistics approach for the downscaling of CMIP5 GCMs for the projection of rainfall in Peninsular Malaysia. J Water Clim Change 11:944–955. https://doi.org/10.2166/WCC.2019.041
O'Neill BC, Kriegler E, Riahi K et al (2014) A new scenario framework for climate change research: the concept of shared socioeconomic pathways. Clim Change 122:387–400. https://doi.org/10.1007/S10584-013-0905-2/TABLES/2
Ooi SH, Samah AA, Braesicke P (2011) A case study of the Borneo Vortex genesis and its interactions with the global circulation. J Geophys Res Atmos. https://doi.org/10.1029/2011JD015991
Paulus A, Shanas S (2017) Atmospheric study of the impact of cold surges and Borneo Vortex over Western Indonesia maritime continent area. J Climatol Weather Forecast 05:1–6. https://doi.org/10.4172/2332-2594.1000189
Peterson P, Funk CC, Landsfeld MF (2015) Precipitation with stations (CHIRPS) v2. 0 dataset: 35 year quasi-global precipitation estimates for drought monitoring. In: AGU fall meeting, pp NH41D-05
Roberts MJ, Camp J, Seddon J et al (2020) Impact of model resolution on tropical cyclone simulation using the HighResMIP-PRIMAVERA multimodel ensemble. J Clim 33:2557–2583. https://doi.org/10.1175/JCLI-D-19-0639.1
Saha S, Moorthi S, Pan HL et al (2010) The NCEP climate forecast system reanalysis. Bull Am Meteorol Soc 91:1015–1057. https://doi.org/10.1175/2010BAMS3001.1

Salimun E, Tangang F, Juneng L et al (2014) Differential impacts of conventional El Niño versus El Niño Modoki on Malaysian rainfall anomaly during winter monsoon. Int J Climatol 34:2763–2774. https://doi.org/10.1002/joc.3873

Samah AA, Babu CA, Varikoden H et al (2016) Thermodynamic and dynamic structure of atmosphere over the east coast of Peninsular Malaysia during the passage of a cold surge. J Atmos Sol Terr Phys 146:58–68. https://doi.org/10.1016/J.JASTP.2016.05.011

Shaaban AJ, Amin MZM, Chen ZQ, Ohara N (2011) Regional modeling of climate change impact on Peninsular Malaysia Water Resources. J Hydrol Eng 16:1040–1049. https://doi.org/10.1061/(asce)he.1943-5584.0000305

Siew JH, Tangang FT, Juneng L (2014) Evaluation of CMIP5 coupled atmosphere-ocean general circulation models and projection of the Southeast Asian winter monsoon in the 21st century. Int J Climatol 34:2872–2884. https://doi.org/10.1002/joc.3880

Smith SA, Vosper SB, Field PR (2015) Sensitivity of orographic precipitation enhancement to horizontal resolution in the operational Met Office Weather forecasts. Meteorol Appl 22:14–24. https://doi.org/10.1002/MET.1352

Suhaila J, Deni SM, Zin WZW, Jemain AA (2010) Spatial patterns and trends of daily rainfall regime in Peninsular Malaysia during the southwest and northeast monsoons: 1975–2004. Meteorol Atmos Phys 110:1–18. https://doi.org/10.1007/s00703-010-0108-6

Sun Y, Ding YH (2010) A projection of future changes in summer precipitation and monsoon in East Asia. Sci China Earth Sci 53:284–300. https://doi.org/10.1007/s11430-009-0123-y

Syafrina AH, Zalina MD, Juneng L (2015) Historical trend of hourly extreme rainfall in Peninsular Malaysia. Theor Appl Climatol 120:259–285. https://doi.org/10.1007/s00704-014-1145-8

Tan ML, Ficklin DL, Ibrahim AL, Yusop Z (2014) Impacts and uncertainties of climate change on streamflow of the johor River Basin, Malaysia using a cmip5 general circulation model ensemble. J Water Clim Change 5:676–695. https://doi.org/10.2166/wcc.2014.020

Tan ML, Gassman PW, Srinivasan R et al (2019) A review of SWAT studies in Southeast Asia: applications, challenges and future directions. Water (Switzerland) 11:914

Tan ML, Juneng L, Tangang FT et al (2020) SouthEast Asia HydrOmeteorological droughT (SEA-HOT) framework: a case study in the Kelantan River Basin, Malaysia. Atmos Res 246:1–12. https://doi.org/10.1016/j.atmosres.2020.105155

Tan ML, Liang J, Hawcroft M et al (2021) Resolution dependence of regional hydro-climatic projection: a case-study for the johor river basin, Malaysia. Water (Switzerland) 13:3158. https://doi.org/10.3390/w13223158

Tangang FT, Juneng L, Salimun E et al (2008) On the roles of the northeast cold surge, the Borneo vortex, the Madden-Julian Oscillation, and the Indian Ocean Dipole during the extreme 2006/2007 flood in southern Peninsular Malaysia. Geophys Res Lett 35:L14S07. https://doi.org/10.1029/2008GL033429

Tangang F, Santisirisomboon J, Juneng L et al (2019) Projected future changes in mean precipitation over Thailand based on multimodel regional climate simulations of CORDEX Southeast Asia. Int J Climatol 39:5413–5436. https://doi.org/10.1002/JOC.6163

Tangang F, Chung JX, Juneng L et al (2020) Projected future changes in rainfall in Southeast Asia based on CORDEX–SEA multimodel simulations. Clim Dyn 55:1247–1267. https://doi.org/10.1007/s00382-020-05322-2

Tao W, Huang G, Lau WKM et al (2020) How can CMIP5 AGCMs' resolution influence precipitation in mountain areas: the Hengduan Mountains? Clim Dyn 54:159–172. https://doi.org/10.1007/s00382-019-04993-w

Titchner HA, Rayner NA (2014) The Met Office Hadley Centre sea ice and sea surface temperature data set, version 2: 1. Sea ice concentrations. J Geophys Res Atmos 119:2864–2889. https://doi.org/10.1002/2013JD020316

Vannière B, Roberts M, Vidale PL et al (2020) The moisture budget of tropical cyclones in HighResMIP models: large-scale environmental balance and sensitivity to horizontal resolution. J Clim 33:1–51. https://doi.org/10.1175/jcli-d-19-0999.1

Volosciuk C, Maraun D, Semenov VA, Park W (2015) Extreme precipitation in an atmosphere general circulation model: impact of horizontal and vertical model resolutions. J Clim 28:1184–1205. https://doi.org/10.1175/JCLI-D-14-00337.1

Wong CL, Venneker R, Uhlenbrook S et al (2009) Variability of rainfall in Peninsular Malaysia. Hydrol Earth Syst Sci Discuss 6:5471–5503. https://doi.org/10.5194/hessd-6-5471-2009

Yang GY, Slingo J, Hoskins B (2009) Convectively coupled equatorial waves in high-resolution Hadley Centre climate models. J Clim 22:1897–1919. https://doi.org/10.1175/2008JCLI2630.1

Yatagai A, Krishnamurti TN, Kumar V et al (2014) Use of APHRODITE rain gauge-based precipitation and TRMM 3B43 products for improving asian monsoon seasonal precipitation forecasts by the superensemble method. J Clim 27:1062–1069. https://doi.org/10.1175/JCLI-D-13-00332.1

Zou L, Zhou T (2015) Asian summer monsoon onset in simulations and CMIP5 projections using four Chinese climate models. Adv Atmos Sci 32:794–806. https://doi.org/10.1007/s00376-014-4053-z